TECHNOLOGY DEVELOPMENT CENTER NEWS

NATIONAL INSTITUTE OF INFORMATION AND COMMUNICATIONS TECHNOLOGY

Serial No. 29   **October 2008**

CONTENTS

The 7th NICT IVS-TDC Symposium

Hiroshi Takiguchi[1] (*htaki@nict.go.jp*) **and Yasuhiro Koyama**[2]

[1] *Space-Time Standards Group, Kashima Space Research Center, National Institute of Information and Communications Technology, 893-1 Hirai, Kashima, Ibaraki, 314-8501, Japan*
[2] *Space-Time Standards Group, National Institute of Information and Communications Technology, 4-2-1 Nukui-Kitamachi, Koganei, Tokyo, 184-8795, Japan*

The 7th IVS (International VLBI Service for Geodesy and Astrometry) TDC (Technical Development Center) symposium held in Kashima Space Research Center (KSRC) of NICT on 15th February 2008. This symposium is held every year as a place in which the VLBI researcher exchanges the result of research and progress information. This time, 19 oral presentations and 1 poster presentation were made at 4 sessions ("Data Analysis and Software Development", "System Development", "Time and Frequency Transfer", "e-VLBI"). Especially, there were 6 presentations from the student of the Yokohama National University, that were the wonderful presentation summarized as a master thesis. There was 29 person participation from the main organizations which do the following VLBI researches. Geograhical Survey Institute, National Astronomical Observatory, National Institute of Polar Research, Yokohama National University, and NICT.

In each session, the interesting topics were presented. Especially, the Q and A session about the presentation of the KARAT which is a software to provide precise ray-tracing results of the atmospheric delay using numerical weather model, the status of development of the very small VLBI system named MARBLE, the ultra rapid UT1 estimation using high-speed network, and the plan to make VLBI array from four over 30m aperture antennas of Ibaraki prefecture by using high-speed network was active. And also the extra explanation of the modified 2.4m antenna was held at the lunch time.

We would like to thank all participants for the contribution to fruitful symposium. Here we have 8 papers in the proceedings. It would be our pleasure if they are useful to many persons. The materials of these presentations are available on the web at `http://www2.nict.go.jp/w/w114/stmp/ivstdc/sympo080215/twmemo7.html` (*in Japanese*).

A Comparison between Current Mapping Functions and Ray-traced Slant Delays from JMA Mesoscale Numerical Weather Data

Ryuichi Ichikawa[1] (*richi@nict.go.jp*),
**Thomas Hobiger[1], Yasuhiro Koyama[1,2],
and Tetsuro Kondo[1,3]**

[1]*Kashima Space Research Center, National Institute of Information and Communications Technology, 893-1 Hirai, Kashima, Ibaraki 314-8501, Japan*
[2]*Space-Time Standards Group,Kashima Institute of Information and Communications Technology, 4-2-1, Nukui-Kitamachi, Koganei, Tokyo 184-8795, Japan*
[3]*Department of Space Survey and Information Technology, Ajou University, Republic of Korea*

Abstract: We have estimated atmospheric slant delays using the KAshima RAytracing Tools (KARAT) through the JMA 10 km MANAL data. The comparisons between KARAT-based slant delays and empirical mapping functions indicate large biases ranging between 18 and 90 mm for summer season, which are considered to be caused by a significant variability of water vapor. We also compared PPP processed position solution using KARAT with that using the latest mapping function for the two week GEONET data sets. The KARAT solution were almost identical to the solution using GMF with linear gradient model, but some cases were slightly worse under the extreme atmospheric condition. Though we need further investigations to evaluate the capability of KARAT to reduce atmospheric path delays under the various topographic and meteorological regimes, the KARAT will be the powerful tool to reduce atmospheric path delay with the numerical weather model improvement.

1. Introduction

We have developed a new tool to obtain atmospheric slant path delays by ray-tracing through the meso-scale analysis data for numerical weather prediction developed by Japan Meteorological Agency (JMA) with 10 km horizontal resolution[4] (hereafter, we call this "JMA 10km MANAL data"). These data is operationally used for the purpose of weather forecast and considered for our study. We have created ray-tracing routines and named the tools "KAshima RAytracing

Tools (KARAT)"[4]. First, we compared empirical mapping functions, developed space geodesy, with KARAT slant delays. Next, we carried out a preliminary comparison between position repeatabilities of precise point positioning (PPP) estimates using KARAT and those using the latest mapping function.

2. KARAT

KARAT have been developed at the National Institute of Information and Communications Technology (NICT), Japan and is capable of calculating total slant delays and ray-bending angles. We perform a successive 19 months run of KARAT calculations from March 2006 to September 2007. The JMA 10km MANAL data which we used in our study provides temperature, humidity, and pressure values at the surface and at 21 pressure levels (which are equal to steps of several meters to kilometers up to about 31 km), for each node in a 10 km by 10 km grid that covers all Japanese islands, the surrounding ocean and Eastern Asia[8]. Figure 1 shows the distribution of the total zenith delays retrieved from the JMA 10-km MANAL data at 1600 UT of July 22nd, 2006.

We first resample the original JMA grid to a modified grid which allows to run the new ray tracing algorithms using analytic expressions. At present the 3-hourly operational products are only available by JMA. Thus, a linear time interpolation is used to obtain results at arbitrary epochs what allows also to evaluate temporal change of estimates. The details of KARAT is described in another paper[4].

3. Comparison between Mapping Functions and KARAT

We compare empirical mapping functions developed for GPS and VLBI with equivalent slant delays estimated by KARAT. Modern mapping functions such as the Isobaric Mapping Function (IMF)[6], Global Mapping Function (GMF)[2], and Vienna Mapping Function (VMF)[1] have been successfully used to estimate site dependent zenith delays in the past few years. The lateral spatial variation of wet delay is reduced by linear gradient estimation. However, the mapping function errors associated with the lateral heterogeneity of the atmosphere have not been assessed sufficiently so far. Our aim is to see how well the modern anisotropic mapping functions can mimic the directional variability associated with the intense mesoscale disturbances typical of the Japanese monsoon.

Figure 2 shows the three typical mapping functions (NMF, VMF, GMF) for station Kashima (a location is shown in Figure 1), Japan from 2005 to

Table 1. *Mean bias and standard deviation values of slant delay residuals in millimeter at elevation of 5° for 16 IGS stations in the East Asia region.*

| IGS	VMF-KARAT	GMF-KARAT	NMF-KARAT
YSSK	-8.3±18.7	-10.8±30.6	-14.1±32.3
MIZU	16.1±43.6	21.9±50.1	31.3±51.0
TSKB	12.3±48.8	22.6±52.7	38.4±53.4
KSMV	8.9±45.0	19.0±49.6	34.7±50.2
KGNI	20.7±44.9	27.3±49.7	43.7±50.1
MTKA	17.9±44.1	25.4±48.4	41.9±48.8
USUD	56.9±32.1	1.6±35.1	12.1±35.5
BJFS	13.6±37.7	14.6±42.4	24.8±42.9
DAEJ	16.4±64.6	18.9±68.7	36.5±69.7
SUWN	-0.6±54.0	4.0±59.4	20.0±59.3
AIRA	-78.5±65.4	-93.9±63.1	-82.1±63.0
GMSD	6.5±50.2	0.5±53.4	25.2±54.9
CCJM	15.8±65.0	2.5±66.0	28.4±66.7
TWTF	21.5±79.7	5.3±80.0	42.5±81.4
TCMS	63.5±93.3	53.8±92.9	92.9±94.1
TNML	63.5±93.3	53.9±92.9	93.0±94.1
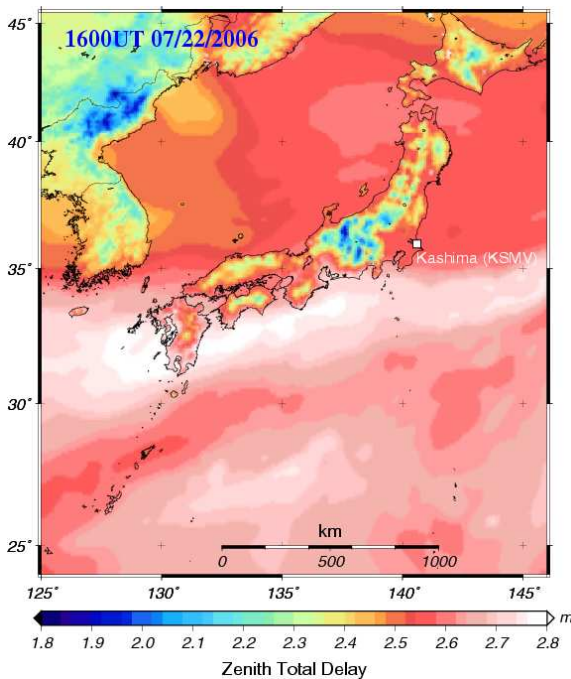
Figure 1. *Zenith total delay retrieved by the JMA 10km MANAL data at the 1600UT of July 22, 2006.*

Figure 2. *Mapping functions VMF (red, thin solid), GMF (blue, dash-dot), and NMF (green, solid) for 5° elevation at Kashima, Japan (IGS station: KSMV), from 2005 to the middle of 2008.*

the middle of 2008. The Niell Mapping Function (NMF) (Niell, 1996) is still widely used by many geodesists. Because it depends only on the station latitude, height and the day of the year, users can easily apply it within data processing without in-situ meteorological measurements. However, NM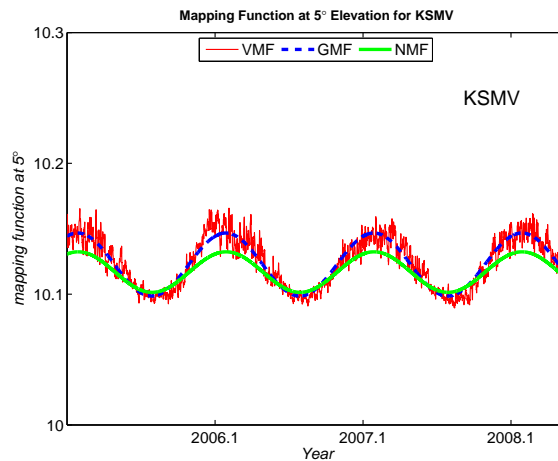F has significant scale biases reaching values up to 0.015 at an elevation of 5° in winter-spring season in eastern Asia region as compared to VMF and GMF, shown in Figure 2. Such biases can lead to significant station height errors.

On the other hand, both GMF and VMF are considered to be globally available to reduce atmospheric path delays for GNSS and VLBI processing. In order to assess the availability of these mapping functions in the East Asia region, we compared KARAT-based slant delays at elevation of 5° from the end of June to September, 2007 with each mapping function values at 16 IGS stations.

We examined both the mean and standard deviation of slant delay residuals. The mean value represents a bias associated with each mapping function, whereas the standard deviation value represents the scatter due to horizontal variability of atmosphere (mainly caused by water vapor variation). The results are summarized in Table 1 and one example histogram of the residuals at Kashima is shown in Figure 3.
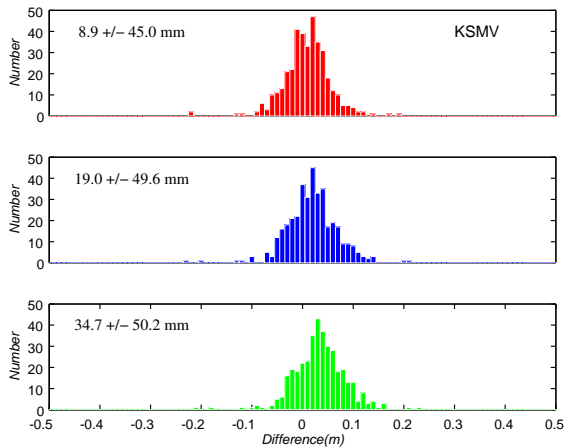

Figure 3. Histogram of residuals in slant delays at elevation of 5° from the end of June to September, 2007. Values between VMF and KARAT (upper), those between GMF and KARAT (middle), and those between NMF and KARAT (lower) are shown, respectively.

Numerical weather model data are based on the physical/dynamical equations that govern the atmospheric flow. The JMA 10 km MANAL data are obtained by combining short model forecasts with new observations (a process called data assimilation). Therefore, the ZTD obtained from KARAT can be considered to be the most realistic empirical value of the real atmosphere.

Large biases of more than 10 mm occur at almost stations, even if VMF is applied. In addition, the scatter of the residuals for all mapping functions is extremely large ranging from 18 to 90 mm, which is caused by significant variability of water vapor. Though these results suggest that the latest mapping functions are insufficient to remove atmospheric path delay in the East Asia region, we need further investigations to understand the behavior of the atmospheric parameters under the various topographic and meteorological regimes.

4. Precise Point Positioning Results for GEONET Stations

In order to compare KARAT processing and empirical mapping functions we analyzed whole data sets of GEONET (GPS Earth Observation Network System), which is a nationwide GPS network operated by Geographical Survey Institute (GSI). In our comparison about 1360 stations of GEONET data during July 9th - 23rd of 2007 were processed.

At first, precise point positioning (PPP) estimates covering the whole period shown above were obtained for all sites using GPSTOOLS[9]. The troposphere delays have been modeled by dry (using the Saastamoinen model[7]) and wet constituents, whereas the latter one were estimated as unknown parameters using the GMF together with linear gradients. The daily position estimates from this solution acts a reference to which the ray-traced solutions can be compared (see Hobiger et al., [2008a] in detail.[3]). In our comparison, PPP estimations using the GMF without linear gradient were also performed.

Changes in the mapping functions primarily cause changes of the station heights in general. According to Hobiger et al.[3], the KARAT solutions are better than the solutions using GMF with gradient during a period of 4 months. In our comparison, the averaged vertical repeatabilities of all solutions demonstrate a similar nation-wide pattern as shown in Figure 4. The largest repetabilities more than 10 mm, which occur in Kyushu and Shikoku islands which are located in the west of Japan, are reflected in all three figures. In addition, Figure 5, which shows the repetabilities for each coordinate component (i.e. the north, east, and vertical errors) for all three solutions, indicates that the KARAT solution is slightly worse than the GMF with gradient solution. On the other hand, KARAT solution is better than the GMF without gradient solution for horizontal component.

During the whole processed period both Kyushu and Shikoku islands have undergone severe heavy rain fall event due to the Baiu front and the typhoon "MAN-YI" passing and cumulating in precipitation amounts ranging 500 - 1100 mm. The time-resolution of the JMA 10km MANAL data is three hours, whereas the PPP processing including gradient estimation was performed for 300 seconds interval. Under the extreme atmospheric condition such as the concerned period, out results imply that the performance of KARAT is almost equal to the solution using the GMF with gradient. We need to extend the processing period for our comparison in order to evaluate a KARAT capability in a reduction of atmospheric path delay.
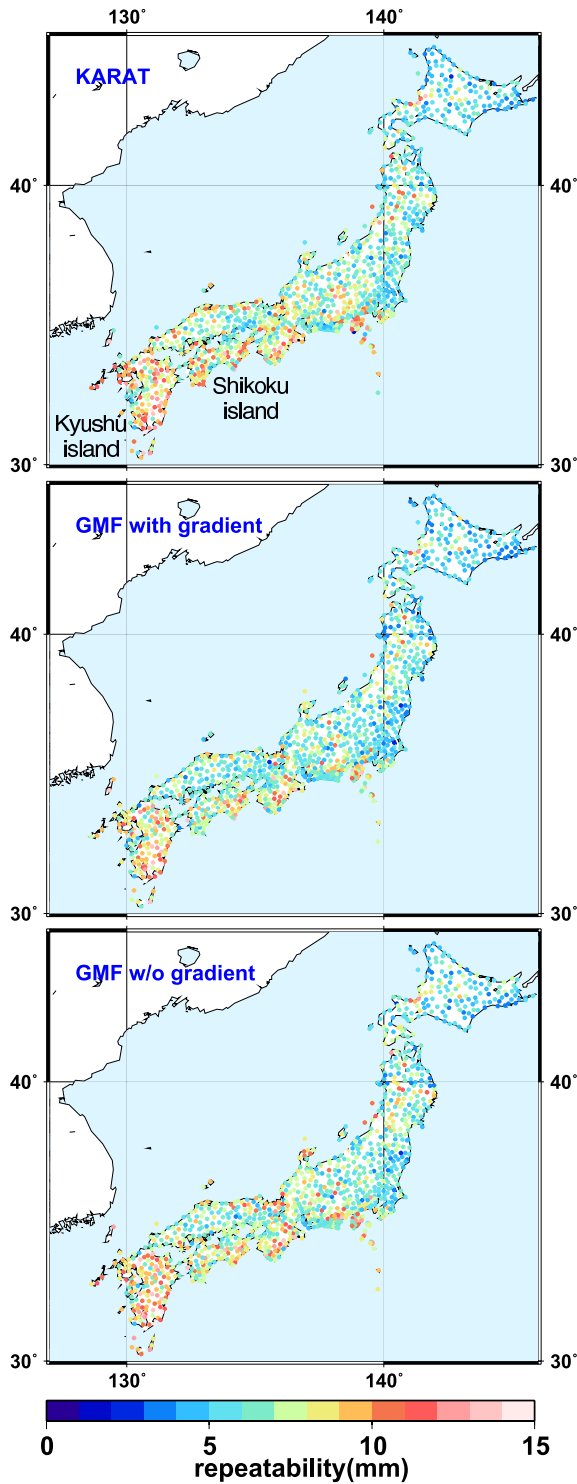
Figure 4. Averaged repeatabilities of station height components between July 9th - 23rd of 2007 for all GEONET stations. The upper represents the solution using KARAT, the middle represents the solution using GMF with gradient, and the lower represents the solution using GMF without gradient.
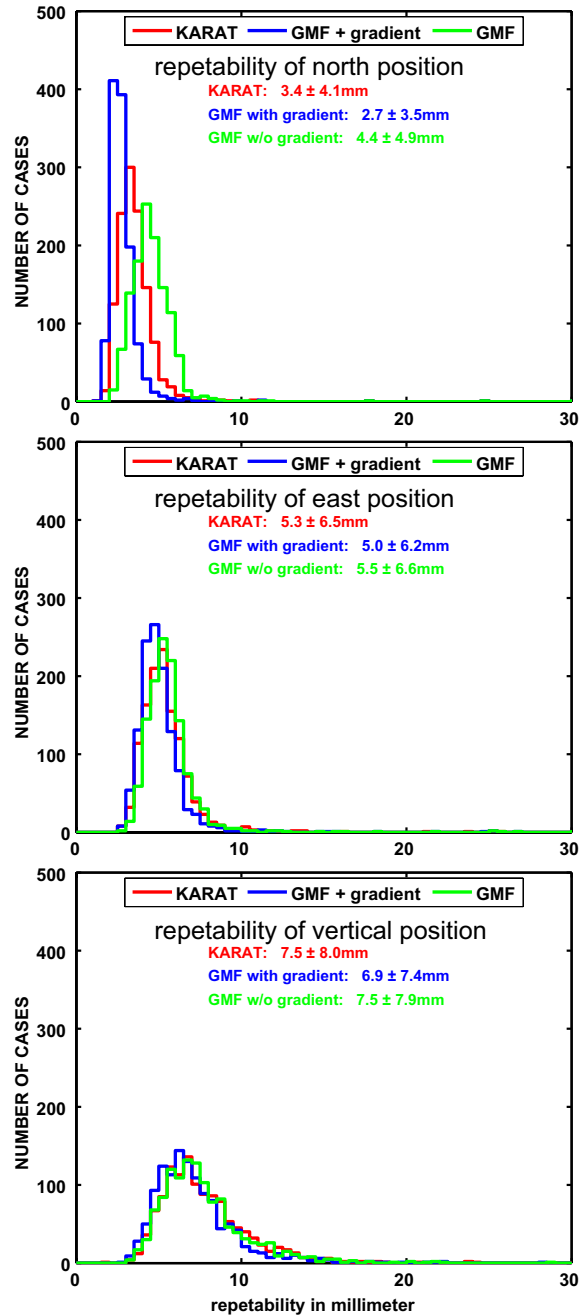

Figure 5. Histogram of repeatabilities for each coordinate component (north, east, and vertical) for each solution.

The advantage of KARAT is an efficient reduction of atmospheric path delay with the numerical weather model improvement (i.e. time and spatial resolution, including new observation data). In spite of the present model imperfectness and coarse time resolution, we hope KARAT will liberate station position determination from numerical instability of unknown parameters.

5.   Summary and Outlook

We have estimated atmospheric slant delays using the KAshima RAytracing Tools (KARAT) through the JMA 10 km MANAL data. The comparisons between KARAT-based slant delays and empirical mapping functions from the end of June to September of 2007 indicate large biases ranging between 18 and 90 mm, which are considered to be caused by a significant variability of water vapor. Next, we compared PPP processed position solution using KARAT with that using the latest mapping function for the two week GEONET data sets. The KARAT solution were almost identical to the solution using GMF with linear gradient model, but some cases were slightly worse under the extreme atmospheric condition. Though we need further investigations to evaluate the capability of KARAT to reduce atmospheric path delays under the various topographic and meteorological regimes, the KARAT will be the powerful tool to reduce atmospheric path delay with the numerical weather model improvement.

References

[1] Boehm, J. and H. Schuh, Vienna Mapping Functions in VLBI analyses, *Geophys. Res. Lett., 31*, L01603, doi:10.1029/2003GL018984, 2004.

[2] Boehm, J., B. Werl and H. Schuh, Troposphere mapping functions for GPS and very long baseline interferometry from European Centre for Medium-Range Weather Forecasts operational analysis data, *J. Geophys. Res., 111*, B02406, doi:10.1029/2005JB003629, 2006.

[3] Hobiger, T., Ichikawa R., Takasu T., Koyama Y., and Kondo T., Ray-traced troposphere slant delays for precise point positioning, *Earth Planets Space, 60*, e1–e4, 2008a.

[4] Hobiger, T., R. Ichikawa, Y. Koyama and T. Kondo, Fast and accurate ray-tracing algorithms for real-time space geodetic applications using numerical weather models, *J. Geophys. Res.*, under review, 2008b.

[5] Niell, A. E., Global mapping functions for the atmosphere delay at radio wavelengths. *J. Geophys. Res., 101*, 3227-3246, 1996

[6] Niell, A. E., A. J. Coster, F. S. Solheim, V. B. Mendes, P. C. Toor, R. B. Langley, and C. A. Upham, Comparison of measurements of atmospheric wet delay by radionsonde, water vapor radiometer, GPS, and VLBI, *J. Atmos. Oceanic Technol., 18*, 830-850, 2001.

[7] Saastamoinen, J., Contributions to the theory of atmospheric refraction, part 2, *Bull. Géodésique, 107*, 13-34, 1972.

[8] Saito, K., et al., The Operational JMA Nonhydrostatic Mesoscale Model, *Monthly Weather Review, 134*, 1266-1298, 2006.

[9] Takasu, T. and S. Kasai, Evaluation of GPS Precise Point Positioning (PPP) Accuracy, *IEIC Technical Report, 105(208)*, 40-45, 2005.

Integer least-squares adjustment for VLBI

Thomas Hobiger (*hobiger@nict.go.jp***),**
Mamoru Sekido, Yasuhiro Koyama,
and Tetsuro Kondo

Kashima Space Research Center, National
Institute of Information and Communications
Technology, 893-1 Hirai, Kashima, Ibaraki
314-8501, Japan

Abstract: Teunissen (1996) presented an algorithm which considers the integer nature of unknown parameters within least-squares adjustment. This method has been successfully applied within GNSS analysis where it helps to solve phase ambiguities. For this study the algorithm has been adopted to the needs of VLBI data processing and applied to simulated and real VLBI data. In particular, it is shown how this algorithm improves the estimation of ambiguities for next-generation VLBI (VLBI2010) and it is discussed how it can be used for the automated phase delay connection of fringe phase data.

1. Introduction

VLBI observables are, similar as GPS measurements, biased by an unknown but quantized number of ambiguities which have to be resolved within post-processing steps. Since sophistcated and straight-forward algorithms are existing for ambiguity resolution of GPS phase observations, we have tried to apply these methods to VLBI. By two examples we show how integer estimation methods can be applied to next-generation VLBI (VLBI2010) data using simulated observations which were generated according to the design specifications of upcoming systems. Additionally we reveal that the same method can be successfully applied to the connection of fringe-phases between consecutive scans.

2. Integer ambiguity estimation in least-squares adjustments

Teunissen (1995[10],1996[8]) presented an algorithm, called Least-squares AMBiguity Decorrelation Adjustment (LAMBDA), which allows the minimization of the a objective function

$$\min ||\mathbf{y} - \mathbf{Bb} - \mathbf{Aa}||^2_{\mathbf{Q_y}^{-1}}$$
$$\text{where } \mathbf{b} \in \mathbb{R}^n \text{ and } \mathbf{a} \in \mathbb{Z}^m \tag{1}$$

and also incorporates variance-covariance information of the observations y. The solution of this problem is obtained in three steps: a least squares-adjustment, ignoring the presence of integer unknowns; the integer ambiguities **a** are estimated using the variance-covariance information from the "float" adjustment; and the "fixed solution", which is the final solution, is computed assuming that the integer values have been resolved correctly.

3. Example 1: Integer ambiguity estimation for VLBI2010-like data

For the purpose of this discussion, VLBI measurements provide two primary types of observation types, those being delays and phases. The former are not affected by ambiguities while the latter are. For any given source, the measured delay $\tau^*_{i,j}(t_k)$ on baseline i, frequency f_j and epoch t_k can be written as

$$\tau^*_{i,j}(t_k) = \tau_i(t_k) + \frac{E_i(t_k)}{f_j^2} + \frac{\partial \tau_i(t_k)}{\partial \alpha} \Delta \alpha_j$$
$$+ \frac{\partial \tau_i(t_k)}{\partial \delta} \Delta \delta_j + \tau^\varepsilon_{i,j}(t_k). \tag{2}$$

where the non-dispersive delay is denoted by $\tau_i(t_k)$, the ionosphere contribution (proportional to the slant total electron content) by $E_i(t_k)$, the random noise of the receiving system by $\tau^\varepsilon_{i,j}(t_k)$, and the "core-shifts" (e.g. *Fey and Charlot* (1997)[2], *Petrachenko and Berube* (2007)[6]) by the third and fourth terms. Although instrumental delays may be of concern, they are beyond the scope of this analysis. It is anticipated that their effect can be adequately reduced through direct and self-calibration processes. Phase measurements, in cycle units, can be written in a similar way by

$$\phi^*_{i,j}(t_k) = f_j \tau_i(t_k) - \frac{E_i(t_k)}{f_j} + f_j \frac{\partial \tau_i(t_k)}{\partial \alpha} \Delta \alpha_j$$
$$+ f_j \frac{\partial \tau_i(t_k)}{\partial \delta} \Delta \delta_j + N_{i,j}(t_k) + \phi^\varepsilon_{i,j}(t_k) \tag{3}$$

where the ambiguity term, denoted by $N_{i,j}(t_k)$, has been introduced. Although it is possible to estimate all the unknowns using a standard Gauss-Markov type least-squares adjustment (e.g. *Koch* (1997)[4]), it is more straightforward to incorporate the added information that the ambiguity values are integer numbers. In the VLBI case, the algorithm will solve for $\tau_i(t_k)$, $E_i(t_k)$, $\Delta \alpha_j$ and $\Delta \delta_j$ as float unknowns and the ambiguities $N_{i,j}(t_k)$ are obtained as integer parameters. For the simulations described in later in this section the MLAMBDA implementation of the algorithm (*Chang* (2005)[1]) has been used. This algorithm works is a similar way to the original LAMBDA method but is superior with respect to computation speed.

The most rigorous approach to resolving the unknown phase cycles (ambiguities) would incorporate all scans that observe the same source into a single least-squares adjustment, as described in section 2.. But this strategy is not feasible for two reasons. Firstly, since the ambiguity search space (*Teunissen et al.* (1996)[8]) grows with each unknown, and the number of ambiguity terms can be large, it becomes nearly impossible to resolve all ambiguities in a reasonable computation time. Secondly, the core-shift terms ($\Delta\alpha_j$ and $\Delta\delta_j$) are highly correlated (> 0.95) with the delay and ionosphere terms, causing the inversion of the variance-covariance matrix to fail or contain elements with unrealistic values, which in turn distorts the integer search algorithm such that the search domain is extended to an incorrect region. In the absence of the core-shift terms, this problem would not exist since each group of frequency related observations become independent and can be treated separately. However, in order to take advantage of the integer ambiguity adjustment methods and to simultaneously estimate the core shifts, a sequential iterative algorithm (*Hobiger et al.*(2008)[3]) is used.

In order to verify the algorithms discussed in the prior section, artificial (simulated) observations have been created. In general, each scan was assumed to consist of measurements from four different bands (with center frequencies set to 2.5,5.25, 7.0 and 11.25 GHz and a 1 GHz bandwidth per subband) what leads to eight observables (four delays and four phases) per scan. In total 233 scans, observing a common source, were taken and the artificial observations were created assuming a signal-to-noise-ratio (SNR) of 14 for all scans, at first. The noise contributions $\tau_{i,j}^{\varepsilon}(t_k)$ and $\phi_{i,j}^{\varepsilon}(t_k)$ were obtained from a Gaussian random generator with zero mean and variances of

$$\sigma_\tau^2 = \frac{12NB}{4\pi^2 SNR^2 BW^2} \ \text{ and } \ \sigma_\phi^2 = \frac{NB}{4\pi^2 SNR^2} \quad (4)$$

where BW reflects the bandwidth, NB stands for the number of frequency bands (i.e. 4) and SNR denotes the overall signal-to-noise ratio, which corresponds to the multi-band delay error. The number of iterations was set to 100 in order to check the performance and behavior of the integer ambiguity resolution strategy. Moreover the number of included observations has been varied between 4, which is the minimum number of observations that provide an overdetermined system, and the maximum number of scans (i.e. 233). Since the algorithm is not depending on the observation geometry, the introduction of a new baseline is expected not to distort the estimation process. From a mathematical point of view there might be a correlation between scans from a single baseline when the time-
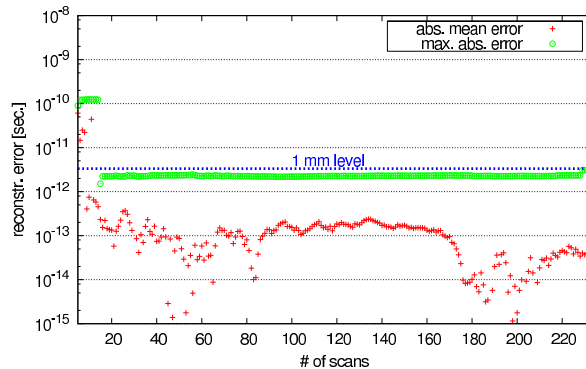

Figure 1. Absolute mean differences (for SNR 14, after 100 iterations, red crosses) between the simulated and the recovered delays in dependence of the number of observations included in the estimation algorithm. The green boxes denote the maximum absolute error in dependence of the number of included scans. The blue dashed line reflects one mm-error level.

span between these observations is small. But as soon as other baselines or further epochs are introduced theses correlations will get smaller and finally dissolve. As shown by *Hobiger et al.*(2008)[3] the correct integer value is found after one or two iterations and further iterations don't lead to the introduction of wrong ambiguities. A slightly larger number of iterations, which is needed in some of the cases, is caused by exceptional large random components. As soon as more observations are included the effect diminishes and the algorithm performs well. In order to verify that the delays are recovered correctly, the absolute mean differences between the modeled and estimated values after 100 iterations are plotted for a different numbers of baselines in figure 1.

It can be seen that the average delay estimation error is far below the mm-level and that even the absolute maximum error does not exceed this boundary. The plot would look nearly similar when the errors are computed directly after the integer ambiguities have been fixed, but the maximum errors would be slightly bigger. The reason for this is that it takes some iterations more to separate delays, ionospheric effects and source structure effects completely. In order to demonstrate that the integer estimation strategy is superior to conventional least-squares techniques, such a solution has been computed too. But since it is not possible to estimate all parameters in one huge adjustment a similar iterative strategy as for the integer estimation has been applied. The only difference was that instead of the MLAMBDA algorithm a simple nearest-integer operator computes the integer ambiguities from the float solution in each iteration.
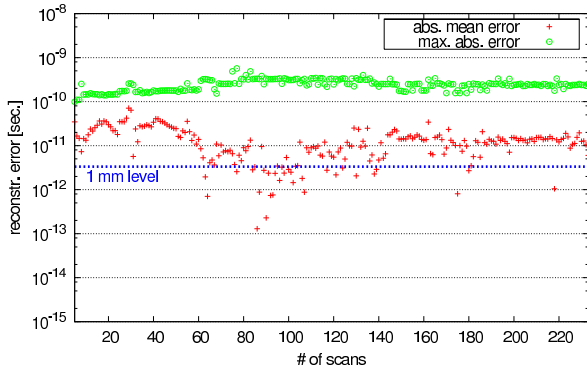
Figure 2. Results from the integer rounding approach (see text). The meaning of the symbols is identical to fig. 3.

Figure 4. Fringe-phases (in cycles) before (blue) and after (green) connection by fitting Cubic-Spline functions (red) together with integer amgiguities. Horizontal axis shows time in seconds.

Figure 2 shows how the recovered delays are differing from the original values after 100 iterations, when the integer rounding strategy is applied.

It is clearly visible that the delays can not be recovered with the same accuracy, even after 100 iterations. Although the absolute mean error is below the one-mm level for a few baseline combinations, the error is on average at the order of 20 ps (7 mm) and the absolute maximum error is around 100 ps (about 3 cm). The reason for the bad performance of the rounding algorithm is due to the fact that even after 100 iterations, the rounding algorithm does not resolve the integer ambiguities correctly (not shown here).

In order to check the behavior of the algorithm for different SNR levels, 730 Monte-Carlo simulated runs (i.e. equal to 2 years of continuous observation) were carried out. Figure 3 shows the averaged ambiguity resolution performance together with the corresponding delay recovery errors.

It can be seen that if the number of scans is larger than 150 all phase cycles can be resolved, down to $SNR_{min} = 12$. If 100 scans are taken only, less than 1% of the ambiguities can not be resolved on average for $SNR \geq 13$. For the cases using 25 and 50 scans it becomes difficult to resolve ambiguities since in some of the runs the core-shifts can not be decorrelated from the other parameters. Thus in the case that the ambiguities are resolved, the mean recovered errors follows exactly the theoretical curves. The equivalent single scan error can be approximated by multiplying the delay recovery errors by $\sqrt{nr_{scan}}$. For 150 and 233 scans it can be verified that the delays per scan can be reconstructed with an error of less than 1.5 ps (0.5 mm) when the SNR is higher than 11. Thus, in order to apply the algorithm in future VLBI processing it is recommended to observe each source more than about 150 times at $SNR \geq 12$ in order
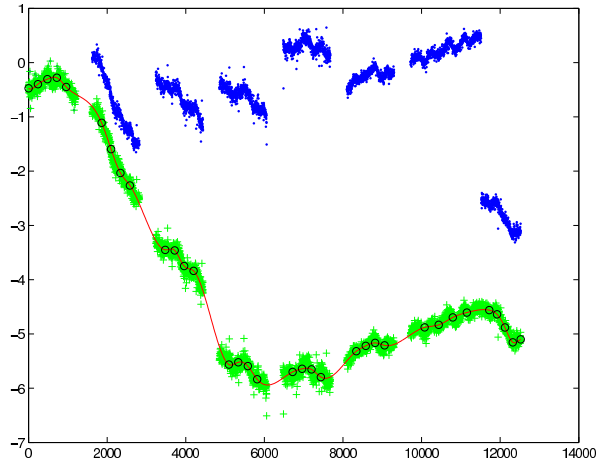
to reliably resolve all the phase ambiguities. Although the algorithm will work in many cases with a a lower number of scans, mathematical correlations between the unknowns can prevent a successful recovery in some of the experiments.

4.   Example 2: Connection of fringe phases between consecutive scans

In order to increase the performance of ΔVLBI observations it is necessary to realiably connect the phase delays (i.e. fringe phases) between consective scans. In our recent studies (*Kondo et al.*(2008)[5]) we have focused on the maximum scan gap limit which permits fringe phase connection. Based on these findings we have tried to apply Teunissen's algorithm, for ΔVLBI. Since the unknown phase cycles are quantized in units of 2π the integer ambiguity algorithm can be used for this problem, too. One has to model the overall phase-delay behaviour by a continous function (e.g. a cubic-Spline function) and estimate the parameters of this function together with the integer ambiguities, which determine the unknown phase cycles of each sub-scan. Figure 4 shows how the algorithm performs for a single-baseline Δ VLBI experiment, tracking a satellite. Ongoing investigations include multi-baseline experiments which allow us to inlcude phase-closure conditions within the adjustment process.

5.   Discussion

It was shown that integer ambiguity estimation is not only useful for GPS, but can also be applied to VLBI. Since the method is based on stochastics it provides the most-likely integer values and thus is
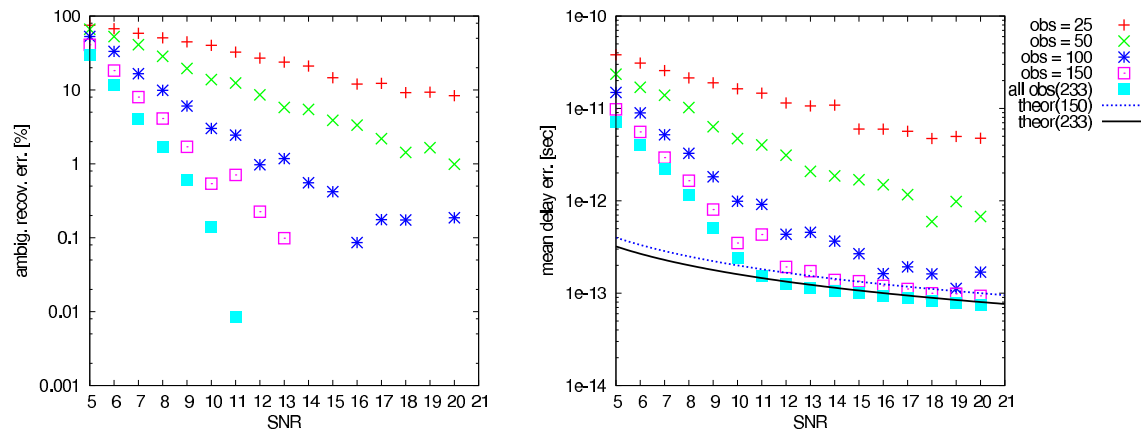
Figure 3. Performance of the integer ambiguity algorithm obtained as mean values from 730 simulated runs, each iterated until the change of the squared sum of improvements of the core-shift positions was less than one $\mu asec^2$. The left figure shows the ratio of unresolved ambiguities in dependency of the SNR level, tested for a different number of observations. The right figure shows the corresponding delay reconstruction error. Additionally the theoretical formal errors for 150 and 233 observations are plotted as reference, whereas it was assumed that phase delays can be referred to a mean frequency of 6.5 GHz.

superior to other algorithms based on rounding or other fuzzy criteria. Moreover the algorithm can be applied to classical least-squares adjustment after small modifications of the algorithms and allows to obtain formal errors of all unknowns, including the integer values.

References

[1] Chang, X.W., X. Yang, and T. Zhou (2005), MLAMBDA: a modified LAMBDA method for integer least-squares estimation, *Journal of Geodesy*, *79*(9), 552–565, doi:10.1007/s00190-005-0004-x.

[2] Fey, A.L. and P. Charlot (1997), VLBA Observations of radio reference frame sources. II. Astrometric suitability based on observed structure, *Astrophys. J. Suppl.*, *111*(95).

[3] Hobiger T., M. Sekido, Y. Koyama and T. Kondo (2008), Integer ambiguity estimation in next-generation geodetic Very Long Baseline Interferometry, Advances in Space Research, accepted, 2008

[4] Koch, K.R. (1997), Parameter Estimation and Hypothesis Testing in Linear Models, Springer, Berlin.

[5] Kondo T., T. Hobiger, M. Sekido, R. Ichikawa, Y. Koyama and H. Takaba (2008), Scan gap limits on phase delay connections in VLBI observations, submitted to Earth, Planets and Space.

[6] Petrachenko B. and M. Berube (2007), VLBI2010 Source Map Alignment Simulation, IVS Memorandum, 2007-008v01, International VLBI Service for Geodesy and Astrometry.

[7] Teunissen, P.J.G. (1995), The least-squares ambiguity decorrelation adjustment: a method for fast GPS integer ambiguity estimation, *Journal of Geodesy*, *70*(1-2), 65–82, doi:10.1007/BF00863419.

[8] Teunissen, P.J.G., P.J. de Jonge and C.C.J.M. Tiberius (1996), The volume of the GPS ambiguity ambiguity search space and its relevance for integer ambiguity resolution, Proc. ION GPS '96, 17-20 September 1996, 889–898.

Development of the software correlator for the VERA system III

Moritaka Kimura (*mkimura@nict.go.jp*)

Kashima Space Research Center,
National Institute of Information and
Communications Technology, 893-1 Hirai,
Kashima, Ibaraki 314-8501, Japan

1. Introduction

The National Institute of Information and Communications Technology (NICT) and the National Astronomical Observatory of Japan (NAOJ) have developed new software correlation system for the VLBI Exploration of Radio Astrometry (VERA) project. Completely same functions as the hardware correlator used in the VERA Project has been attained in the software correlation system. The data rates supplied from each radio telescopes are 1024Mbps. This software correlator has attained the same processing speed as the hardware correlator of the VERA system by only five sets of PC and disk arrays. Some benchmark tests, comparison of the results with the hardware correlator are described in the past TDC news [2]. Some information of the software correlation systems which were not described before introduce this time.

2. Design of the software correlator

The basic design of the VERA software correlator is the same as the K5/VSI correlator named GICO3 developed by NICT [1]. The GICO3 is a correlator of the FX type that processes multi baselines at the same time. Internal block diagrams of the correlation process in the GICO3 is shown in the figure 1 in a simple case of two stations named 'A' and 'B'. In order to achieve high performance, the GICO3 have double buffer at each stations for parallel processing. One buffer is used for file access and another buffer is used for numerical operation. There are one file access thread and some numerical operation threads generated at the same time. Since components of the K5/VSI were chosen so that file access time and numerical operation time may become equal, compared with sequential processing of numerical operations after file access are performed, correlation processing is completed in half time by parallel processing. VLBI observation data named 'raw-file' are converted into the floating point data by using the table lookup algorithm, because floating point operations are necessary to express the internal expression in the correlation process of the FX type correlator. For correlation process of the multi channel observation, a single channel is picked and converted into floating point data at here. Since, the delay tracking and the phase tracking are perform in the frequency space, real-FFT algorithm can be used. As a result, computing time in the FFT becomes half compared with complex-FFT algorithm. The delay tracking and the phase tracking in the frequency space are performed by correcting phase gradient and intercept. In order to exclude the operation of trigonometric functions which need very long processor clocks, the table lookup algorithm of 256 sin-cos elements is used. Auto-correlation and the cross-correlation are calculated at once, and the integrated results are recorded in the correlation output files periodically. A lot of numerical processing are perform by vector operations and some functions are described by assembler language. For this reason, total speed of the GICO3 has attained the same speed as a hardware correlator using five sets of PC.
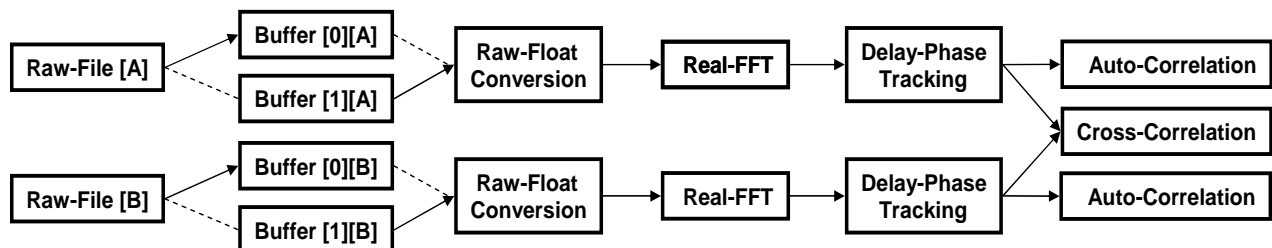

Figure 1. Block diagram of the GICO3 correlator in a case of two stations.

3. The Correlation Schedule of the GICO3

The correlation schedule of the GICO3 is described by the XML language. A new item can be easily added. A simple correlation schedule is described in the following. Specification of some digital backends and translating rules that convert raw-file into floating point value are assigned in "terminal" items. Position of the radio telescopes, the name of a digital backend and a name of the directory which stored observation raw-file are assigned in "station" items. By assigning several different backend name in the "station" items, correlation with mixed digital backend can be possible. The Name of radio source whose position is used for geometric delay calculation, the index which distinguishes a specific A/D channel in the raw-file which have several channels and some information are assigned in the "stream" items. Correlation processing of multi-channel observations and / or multi-beam observations are possible by assigning several streams.

```
<?xml version="1.0" encoding="UTF-8" ?>

<schedule>

  <terminal name="VERA-01">
    <speed>256000000</speed>
    <channel>2</channel>
    <bit>2</bit>
    <level>-1.5,-0.5,+0.5,+1.5</level>
  </terminal>

  <station key="A">
    <name>MIZNAO20</name>
    <pos-x>-3857241.8226</pos-x>
    <pos-y>+3108784.8097</pos-y>
    <pos-z>+4003900.5431</pos-z>
    <terminal>VERA-01</terminal>
    <raw-dir>/mnt/raid/raw-file</raw-dir>
  </station>

  <station key="B">-omission-</station>
  <station key="C">-omission-</station>
  <station key="D">-omission-</station>

  <clock key="A">
    <epoch>2003/328 01:34:00</epoch>
    <delay>+0.000000000</delay>
    <rate> +0.000000000</rate>
    <acel> +0.000000000</acel>
    <jerk> +0.000000000</jerk>
    <snap> +0.000000000</snap>
  </clock>
  <clock key="B">-omission-</clock>
  <clock key="C">-omission-</clock>
```

```
  <clock key="D">-omission-</clock>

  <source name="3C345"  >
    <ra>  16h42m58.80997</ra>
    <dec>+39d48'36.99406</dec>
  </source>
  <source name="NRAO512">-omission-</source>

  <stream>
    <label>CH01</label>
    <source>   3C345</source>
    <frequency>+22220000000</frequency>
    <channel>01</channel>
    <fft-point>2048</fft-point>
    <output-Hz>1</output-Hz>
  </stream>
  <stream>
    <label>CH02</label>
    <source> NRAO512</source>
    <frequency>+22220000000</frequency>
    <channel>02</channel>
    <fft-point>2048</fft-point>
    <output-Hz>1</output-Hz>
  </stream>

  <process>
    <start>2003/328 01:34:00</start>
    <length>3960</length>
    <object>Multi</object>
    <stations>ABCD</stations>
  </process>

  <process>-omission-</process>
  <process>-omission-</process>

</schedule>
```

4. Multi-Beam Correlation

Since the general radio telescope observed only one radio source at once. it is designed so that a correlator may also process one radio source at once. Since the radio telescope used for the VERA project can observe two radio sources at once, the hardware correlator of the VERA project can process two radio sources at once. When a general correlator performs the VERA's two-beam correlation, it is possible by changing radio source positions and performing correlation processing twice, but it is very inefficient. Since there is no necessity that software correlator should perform correlation with fixed processing speed like hardware correlators, it is enables to perform multi-beam correlation whose calculation load are changed dramatically. The GICO3 can perform correlation process at once with many radio source, and it is effective to correlate of the masar spots that spread in the
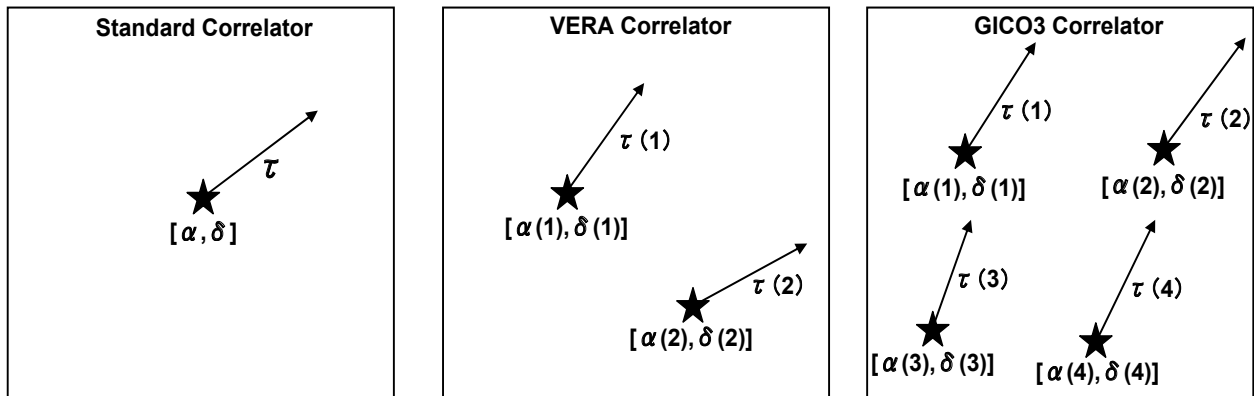
Figure 2. left: the standard correlator performs delay tracking to one radio source position. center: the VERA correlator performs delay tracking to two radio source positions. right: the GICO3 correlator performs delay tracking to many radio source positions.

celestial sphere widely like a figure 2.

5. Conclusion

The software correlation system have started experimental operation in the Mitaka correlator room. Many kinds of operation tests are also completed and same correlation output results as hardware correlation processing is obtained by software correlation system. After carrying out durability test, this system will operate in the part of the VERA correlation system.

References

[1] Kimura, M. , 2-Gbps PC Architecture and Gbps data processing in K5/PC-VSI, IVS CRL-TDC News, No.23, pp.12-13,November 2003

[2] Kimura, M. , Development of the software correlator for the VERA system II, IVS CRL-TDC News, No.28, pp.22-25,November 2007

Figure 3. The K5/VSI system installed in the Mitaka correlator room

Developments of K5/VSI System for Geodetic VLBI Observations

Yasuhiro Koyama (*koyama@nict.go.jp*),
Tetsuro Kondo, Mamoru Sekido,
and Moritaka Kimura

Kashima Space Research Center, National
Institute of Information and Communications
Technology, 893-1 Hirai, Kashima, Ibaraki
314-8501, Japan

Abstract: The developments of the K5 VLBI system started in 1999 and diverse component systems have been developed to support various kinds of VLBI observations and data processing requirements. The main concept of the K5 VLBI system is to realize real-time VLBI observations and correlation processing performed with various observing modes by combining multiple components in a flexible manner. The system is also intended to be compliant with the other VLBI related systems by adopting standardized interfaces. Recently, the K5/VSI Data Recording Terminals and ADS3000+ high speed AD sampler unit have been developed. The details of these newly developed component systems will be described.

1. Introduction

National Institute of Information and Communications Technology (NICT) is one of the technology development centers of the International VLBI Service for Geodesy and Astrometry (IVS), and we have been developing VLBI observation systems and data processing systems to improve the capabilities of the existing systems. In 1999, we started to develop K5 VLBI system, which consists of the PC-based data acquisition terminals and software based correlation processing programs. In contrast to the previous K4 VLBI system developed with the specially designed high speed cassette tape recording system, the K5 VLBI system is designed with the commodity products such as personal computers, hard-disks, and network components. This strategy has been quite successful to develop highly flexible and high performance observation systems and data processing systems for VLBI. As the data acquisition terminals of the K5 system, we have developed two independent series of systems. One is the K5/VSSP system series [Kondo et al., 2003[1]] and the other is the K5/VSI system series [Koyama et al., 2003[2]]. The concept of the K5/VSSP system and its next generation K5/VSSP32 system is to develop AD sampling units interfaced to the commodity PC systems by using the PCI expansion bus (VSSP) and USB2.0 interface (VSSP32). Each AD sampling unit can support up to four analog inputs, and therefore, four units are used to record signals from 16 full channels of baseband converter units in the case of usual geodetic VLBI observations. On the other hand, K5/VSI series are realized by high speed AD sampler units and all of these units are interfaced with the commodity Linux PC systems with the VSI-H (VLBI Standard Interface - Hardware specifications). VSI-H was proposed to define standard interface for the high speed data transfer between data input modules, data transfer modules, and data output modules to improve the compatibility between next generation VLBI observing systems and the correlator systems. To input the data stream from the VSI-H data input modules, a special board called PC-VSI board has been developed. The board is installed to the PCI expansion bus slot of Linux PC system and can support high speed data transfer and recording up to 2Gbps with a single unit. Three data sampler units, ADS1000 [Nakajima et al., 2001[4]], ADS2000 [Koyama et al., 2006[3]], and ADS3000 [Takeuchi et al., 2006[5]], have been developed to support various sampling modes. ADS1000 can sample one baseband channel at the sampling rate of 1024Msps. ADS2000 can sample 16 baseband channels at the sampling rate of 64Msps suitable for observations using the bandwidth synthesis method. ADS3000 can sample wide range of baseband frequency band up to 1024MHz with the sampling rate of 2048Msps. A high speed FPGA (Field Programmable Gate Array) chip is equipped inside the unit and it can be used to process the input data stream for digital filtering and digital baseband conversion processing. By developing specialized program for the FPGA chip, ADS3000 has a potential to support various observing modes without hardware baseband converters.

2. Developments of the K5/VSI Recording Terminal

By using the PC-VSI boards which have been expanded to support 2Gbps data rate and commodity raid controller boards, two racks of the K5/VSI recording terminal have been configured. Figure 1 and Figure 2 are the pictures of the recording terminal taken from the front side and the rear side respectively. One terminal consists of two rack mounted Linux operating PC units and necessary auxiliary components like an LCD display, a keyboard, a mouse, and a switch for these components. Each unit is installed with a PC-VSI board and a raid control board on its PCI expansion bus slots.

Sixteen 1 TByte hard-disks are controlled by the raid control board to configure RAID-0 system. Table 1 lists the detailed components used for the recording unit. Each recording terminal is configured with two of these units.

Figure 1. K5 Recording Terminal (Front View).

Table 1. Components of the K5 Recording Unit.

CPU (2)	Intel Xeon 2.33GHz
Mother Board	Supermicro X7DBE
Raid Controller	Gighpoint RocketRAID 2340
RAM	4 GByte (2 GByte x 2)
HDD (16)	Seagate ST31000340AS
	(1TByte SATA 7200RPM)

With one recording terminal, 32TBytes of total data capacity can be used and the data can be recorded at the data rate of 4.096Gbps by using two VSI-H data input ports. If the data are recorded continuously, the total capacity can support recordings up to 17.36 hours. The capacity is considered to be enough for usual VLBI observations where actual recording time is roughly 50The capacity of the recording terminal can also be enlarged by replacing the hard-disk units if such high volume hard-disks with more than 1TByte of disk capacity become available in the future. Since the
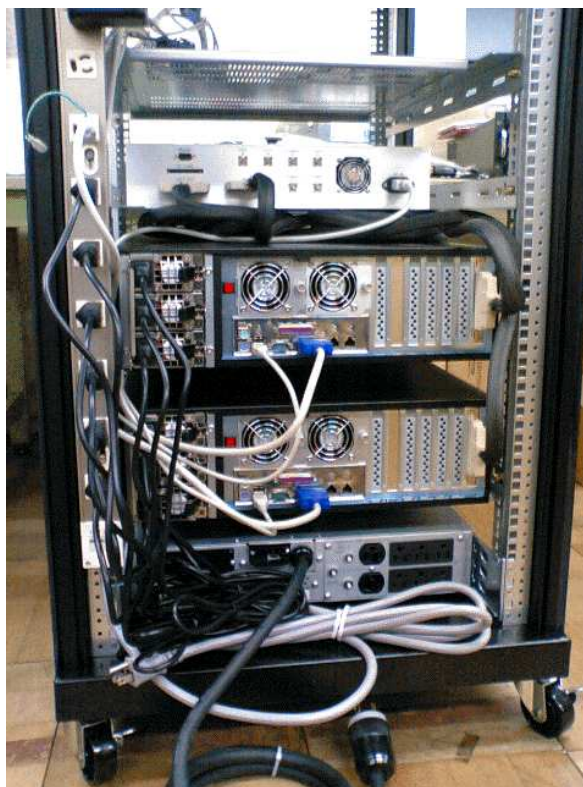
Figure 2. K5 Recording Terminal (Rear View).

commodity raid controller board is used under the Linux PC environment, the data file can be easily accessed from application programs as simple data files on the Linux operating system.

It has to be noted that the reliability of the recording terminal is affected by the performance of the hard-disk modules. Figure 3 shows the recording performance of the system measured by benchmark program for two different hard-disk modules. While the module A (Seagate ST31000340AS) can sustain 4Gbps recording speed from the beginning to the end of the total capacity, intermittent performance degradations were recorded with the module B. Although there are short falls in the recording speed with the module A, such events can be recovered by the data buffer on the hard-disk modules and data loss did not occur at all during several recording tests. The large recording speed falls with the module B were larger than the capacity of the data buffer, and actual data losses occurred. But, even with this configuration, it is worth noted that the recording is maintained with adequate flagging to the data and it is still possible to correlate the data with the other stations' recorded data by suppressing integration to the lost data segments.
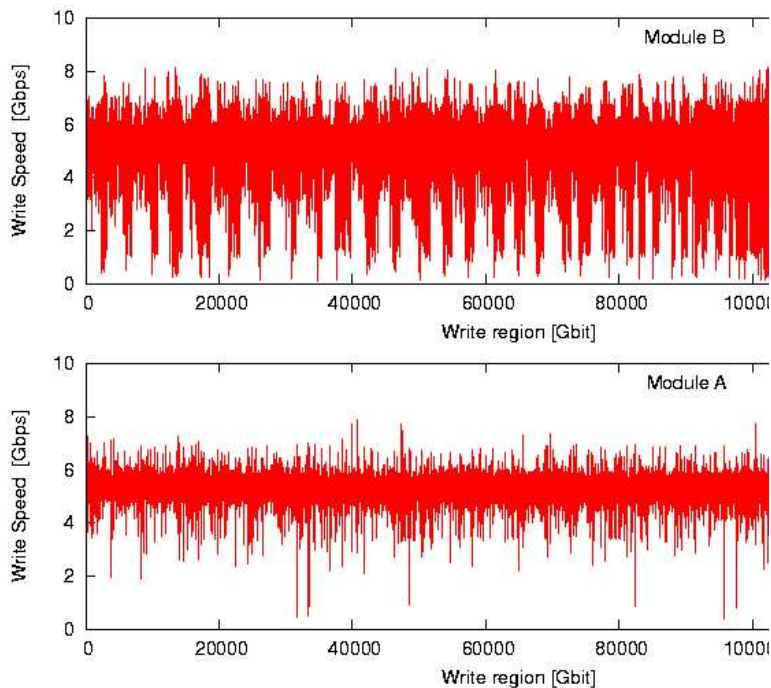
Figure 3. Recording speed performance with hard-disk module A (Seagate ST31000340AS) and module B.

3.   Developments of the ADS3000+

After developing two units of the ADS3000 high speed AD sampler units, we started to extend the capabilities of the ADS3000 system by adopting faster AD sampler chip and two new FPGA chips replacing one FPGA chip. The EV8AQ160 AD sampler chip was recently released from e2V corporation and it has a capability to sample high speed analog data up to 5GHz. The chip can work at the clock rate of up to 2.5GHz and the input signal can be sampled synchronized to the external clock signal and additionally at the timing every half of the timing of the external clock signal. By using this capability, the maximum sampling speed of the ADS3000+ system has become 4096Msps. To process the high speed digital data from the sampler chip, two FPGA chips are used. Two FPGA chips are cascaded on the processing board of the ADS3000+ system. The first stage FPGA chip is used for the processing which require high speed data handling, such as demultiplexing and multiplexing the data, and the second stage FPGA chip is used for the complex data processing, such as digital filtering and digital base-band converter processings. Table 2 shows the major specifications

of the ADS3000+ system. Figure 4 shows the picture of the ADS3000+ system and Figure 5 shows the schematic configuration of the main processing board of the ADS3000+.

Table 2. Specifications of the ADS3000+ unit.

AD chip	e2V EV8AQ160
Size	EIA 2U (480mm x 88mm x 430mm)
Sampling Modes	4096Msps x 1ch
	2048Msps x 2ch
	1024Msps x 4ch (option)
FPGA chip 1	Xilinx Virtex5 XC5VLX110-3
FPGA chip 2	Xilinx Virtex5 XC5VLX220-2

Currently, necessary software programs to be loaded on two FPGA chips are under developments. At beginning, only limited simple function will be realized and ADS3000+ will support simple observing modes, such as 2048Msps 2 IF channels mode and 4096Msps 1 IF channel mode. In the next step, digital filtering and baseband converting programs will be loaded on the second stage FPGA chip to support multiple channel observations. If this capability is realized, currently used hardware
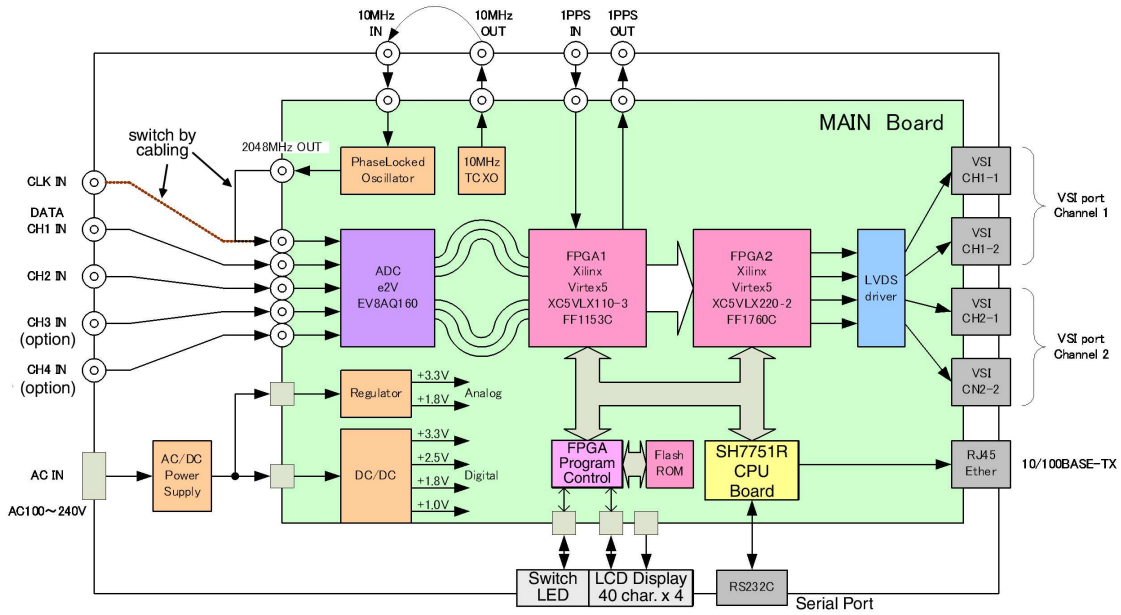
Figure 5. Schematic diagram of the ADS3000+ logic board.

Figure 4.   View from the front side of the ADS3000+ system.

baseband converter units will become unnecessary and the VLBI observing system will become much simpler.

References

[1] Kondo, T., Y. Koyama, J. Nakajima, M. Sekido, and H. Osaki, Internet VLBI system based on the PC-VSSP (IP-VLBI) board, New Technologies in VLBI, ASP Conference Series. **Vol.306**, pp.205-216, 2003.

[2] Koyama, Y., T. Kondo, J. Nakajima, M. Sekido, and M. Kimura, VLBI obser-vation systems based on the VLBI Standard Interface Hardware (VSI-H) specifications, New Technologies in VLBI, ASP Conference Series, **Vol.306**, pp.135-144, 2003.

[3] Koyama, Y., T. Kondo, M. Kimura, M. Hirabaru, and H. Takeuchi, Real-time High Volume Data Transfer and Processing for e-VLBI, Advances in Geosciences, **Vol.6**, Hydrological Science pp.81-90, 2006.

[4] Nakajima, J., Y. Koyama, M. Sekido, N. Kurihara, T. Kondo, M. Kimura, and N. Kawaguchi, 1-Gbps VLBI, the First De-tection of Fringes, Experimental Astronomy, **Vol.11**, pp.57-69, 2001.

[5] Takeuchi, H., M. Kimura, J. Nakajima, T. Kondo, Y. Koyama, R. Ichikawa, M. Sekido, and E. Kawai, Development of 4-Gbps Multi-functional VLBI Data Acquisition System, Publications of the Astronomical Society of the Pacific, **Vol.118**, pp.1739-1748, 2006.

Current Status of Development of a Compact VLBI System for Providing over 10-km Baseline Calibration.

Atsutoshi Ishii (*ishii@nict.go.jp*)[1,2,3],
Ryuichi Ichikawa[2]**, Hiroshi Takiguchi**[2]**,
Hiromitsu Kuboki**[2]**, Tetsuro Kondo**[2]**,
Yasuhiro Koyama**[2]**, Morito Machida**[1]**,
and Shinobu Kurihara**[1]

[1] *Geographical Survey Institute*
   1 Kitasato, Tsukuba, Ibaraki 305-0811, Japan
[2] *Kashima Space Research Center,*
   National Institute of Information and
   Communications Technology, 893-1 Hirai
   Kashima, Ibaraki 314-8501, Japan
[3] *Advanced Engineering Services Co.,Ltd.*
   1-6-1 Takezono, Tsukuba, Ibaraki 305-0032,
   Japan

Abstract: We are developing a compact VLBI system with 1.65 m diameter aperture antenna in order to provide reference baseline lengths for calibration. The reference baselines are used to validate surveying instruments such as GPS and EDM and maintained by the Geographical Survey Institute (GSI). The VLBI system is designed to be assembled with muscle power simply in order to perform short-term (about one week) measurements at several reference baselines in Japan. We plan to use a broad-band dual-polarized antenna for feed horn of this VLBI system. Antenna pattern of this broadband feed horn was measured in an anechoic chamber. Using the measured antenna pattern and antenna analysis software, the optimum F/D of main reflector was estimated. We have also evaluated a front-end system with a broad-band feed horn by installing it on the 2.4 m diameter antenna at Kashima. On December 5 of 2007, we have successfully detected fringes of the 3C84 signal for S/X band using 2.4m antenna and 34m antenna in Kashima.

1.   Introduction

National Institute of Information and Communications Technology (NICT) are developing a compact VLBI system with 1.65 m diameter aperture antenna in collaboration with GSI. GSI has a responsibility to calibrate and validate survey instruments such as GPS receivers and Electro-Optical Distance Meter (EDM). The validation works are operationally carried out at a 10 km reference baseline maintained by GSI, which is located about 5 km east from GSI headquarters, Tsukuba,

Japan. Along the baseline, pillar monuments made of stainless steel are installed. To guarantee the quality of validation, the baseline length has to be examined routinely. However, the entire distance of the reference baseline too long to be measured by a EDM directory, the examination at present are only performed by GPS receiver.

On the other hand, Geodetic VLBI technique can give an independent measurement to examine the baseline with a few millimeters accuracy. Thus, we made idea of the geodetic VLBI system that combined a small antenna and a big antenna for the purpose. This VLBI system is using a pair of very small antennas combined with a large aperture antenna (Figure 1). Those small antennas will be installed at both ends of the reference baseline. However, time delay between small antennas is directly undetectable due to their low sensitivity. Two time delays between each small antenna and the large one can be detected. Time delay between small antennas can be obtained from those time delays indirectly. We named the idea 'Multiple Antenna Radio-interferometry of Baseline Length Evaluation (MARBLE)'.

In this article, we describe development of the compact VLBI system which is the core equipment of MARBLE.

2.   Development

2.1   Compact VLBI System

The main part of the MARBLE system is the compact VLBI system as described so far. To perform short-term (about one week) measurements at several reference baselines in Japan, the most important idea in developing the VLBI system is transportability. The VLBI system consists of a 1.65 m diameter aperture antenna, a front-end unit, a down converter unit, a azimuth drive unit, a elevation drive unit, and etc (Figure 2). The main reflector, the azimuth drive unit, and the elevation drive unit are detachable respectively. These are designed to be assembled without heavy machines. To calibrate ionospheric path delay error, this system can receive the X-band and S-band. A broadband dual-polarized horn antenna (ranging 2 GHz - 18 GHz [2]) made by ETS-Lindgren will be used as a feed horn of this antenna to achieve it. This system can also equip a target marker for local tie measurement in the point of intersection of Az-El drive axes.

2.2   Design and Test The Components

2.2.1   Design The Antenna

The type of antenna of the compact VLBI system was designed to front-fed paraboloid, since the

efficient collection of radio waves with a small aperture and the processing were easy. A paraboloid reflector can be defined by a F/D where F is a focal length and D is a diameter. The optimum F/D of the main reflector of compact VLBI system was estimated as follows method. First of all, the antenna pattern of the feed horn was measured in an anechoic chamber (Figure 4). Based on the measured antenna pattern, the aperture efficiency of front-fed paraboloid was calculated using antenna analysis software GRASP8 [3] with several F/D values. Moreover, a noise from the spillover was considered. Consequently, the estimated optimum F/D was 0.45 to 0.52. Actually, the main reflector which F/D is 0.45 (D=1650mm, F=740mm) was produced as a prototype.

2.2.2 Surface Measurement of The Main Reflector

We measured surface accuracy of the main reflector by using a vision metrology. The vision metrology system that we used is a very simple system that used digital camera and note PC. The measurement accuracy is about 0.1mm on a 2m object. Figure 3 shows state of this measurement. Surface accuracy measured was 0.30mm RMS. It was a good enough compared with the wavelength of X-band.

2.2.3 Evaluation of Front-end System

We produced a new front-end system with broadband feed horn as a prototype. In order to confirm its performance, the new front-end system was installed on the 2.4 m diameter antenna at Kashima (CARAVAN2400 [1]). We carried out the fringe test using CARAVAN2400 and Kashima 34m antenna on December 5 of 2007. We have successfully detected fringes of the 3C84 signal for both S and X bands on December 5 of 2007 (see Figure 5).

3. Conclusion

We are developing a compact VLBI system with 1.65 m diameter aperture antenna in order to provide reference baseline lengths for GPS and EDM calibration maintained by GSI. The antenna of this compact VLBI system was designed based on using the broad-band feed horn. A main reflector was designed with optimum F/D and produced. We also produced a new front-end system with broad-band feed horn. In order to confirm this front-end performance, it was installed on the CARAVAN2400. We successfully detected fringes of the 3C84 signal for both S and X bands using remodeled the CARAVAN2400.

References

[1] Ishii, A., R. Ichikawa, H. Kuboki, Y. Koyama, K. Takashima, and J. Fujisaku, VLBI Experiments Using CARAVAN2400, *IVS NICT-TDC News No.27*, pp.9-13, Aug 2006.

[2] Lindgren, ETS-Lindgren (2005). The Model 3164-05 Open Boundary Quadridge Horn, Data Sheet.

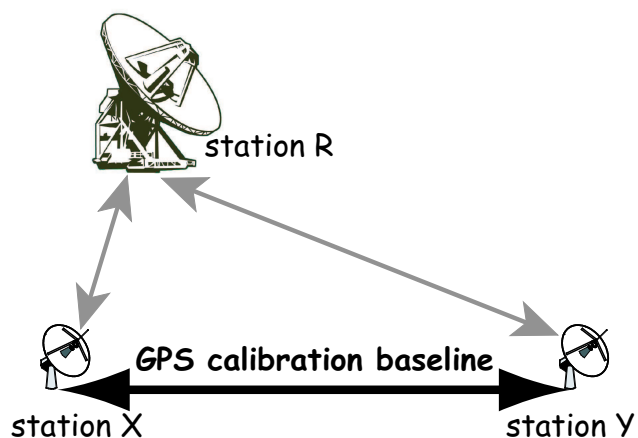[3] Pontoppidan, K., TICRA, Technical Description of GRASP8, Feb 2003.

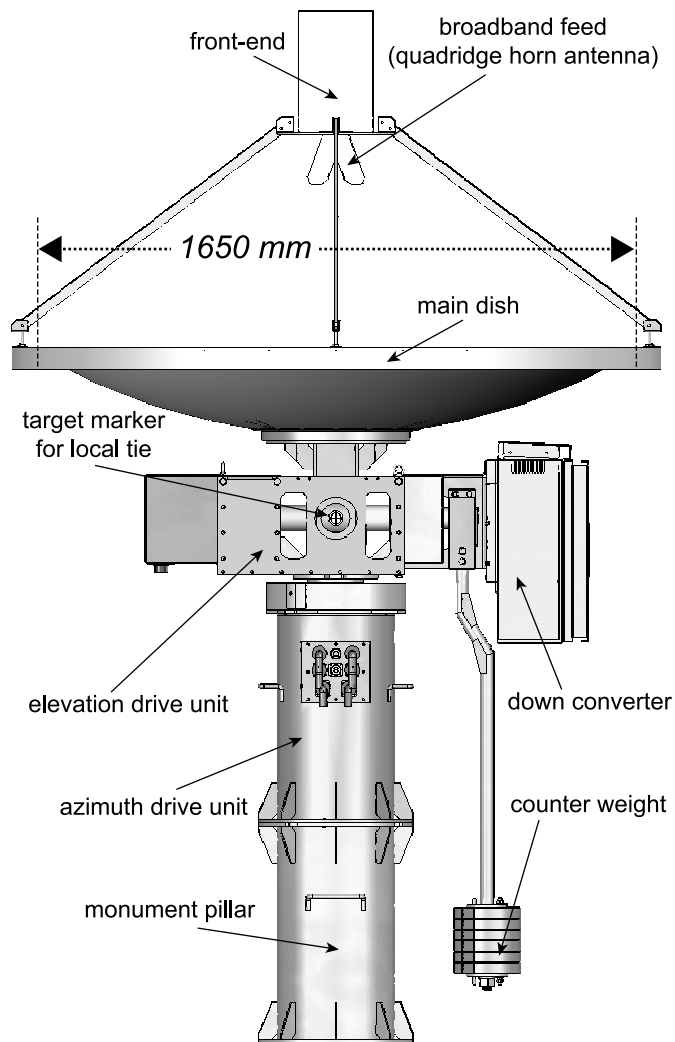*Figure 1. Concept of the length examination for the reference baseline using VLBI technique.*

Figure 2. Schematic image of the MARBLE compact VLBI system.

Figure 3. State of surface measurement of the main reflector.
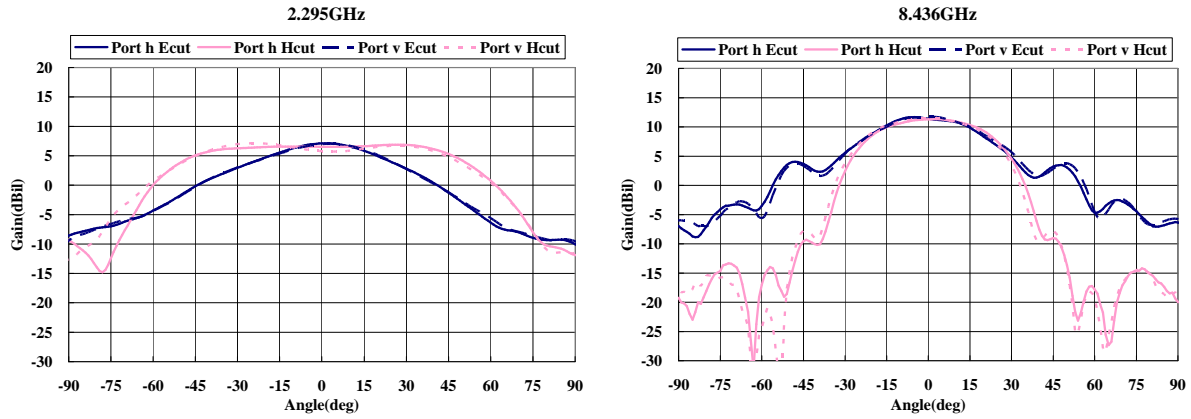
2.295GHz

8.436GHz

Figure 4. Measured antenna patterns of the broad-band feed. Prot v and h are two separate linear polarizations respectively.
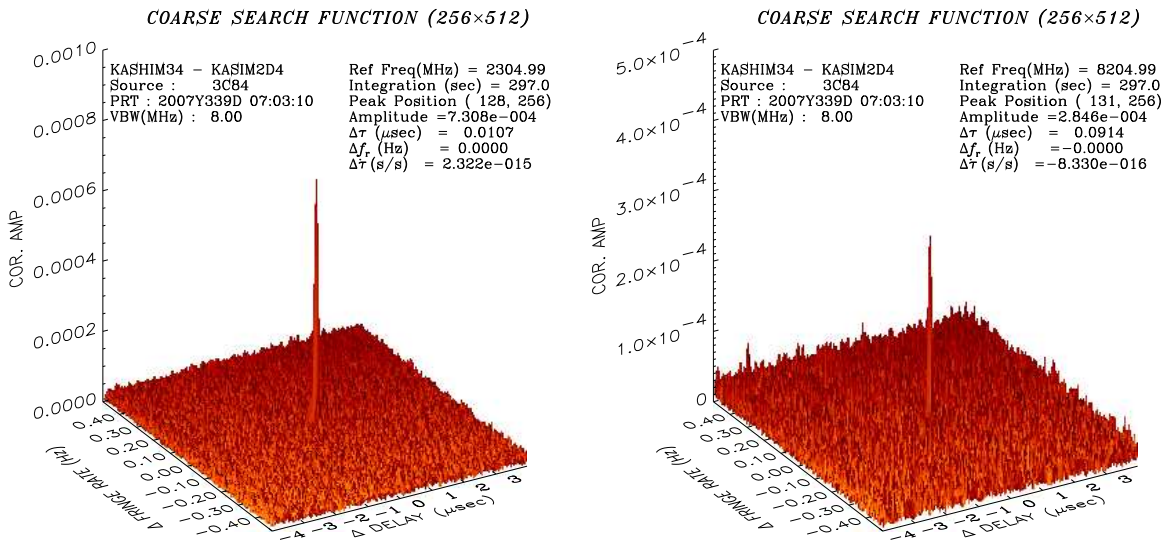

Figure 5. Detected fringes using new front-end.

Comparison Study of VLBI and GPS Carrier Phase Frequency Transfer using IVS and IGS data

Hiroshi Takiguchi[1] (*htaki@nict.go.jp*),
Yasuhiro Koyama[1]**, Ryuichi Ichikawa**[1]**,
Tadahiro Gotoh**[2]**, Atsutoshi Ishii**[1,3,4]**,
Thomas Hobiger**[1]**, and Mizuhiko
Hosokawa**[5]

[1] *Space-Time Standards Group,
Kashima Space Research Center,
National Institute of Information and
Communications Technology,
893-1 Hirai, Kashima, Ibaraki,
314-8501, Japan*
[2] *Space-Time Standards Group,
National Institute of Information and
Communications Technology,
4-2-1 Nukui-Kitamachi, Koganei, Tokyo,
184-8795, Japan*
[3] *Geographical Survey Institute,
1 Kitasato, Tsukuba, Ibaraki,
305-0811, Japan*
[4] *Advance Engineering Services Co., Ltd
1-6-1 Takezono, Tsukuba, Ibaraki,
305-0032, Japan*
[5] *Strategic Planning Department,
National Institute of Information and
Communications Technology,
4-2-1 Nukui-Kitamachi, Koganei, Tokyo,
184-8795, Japan*

Abstract: We compare the frequency transfer precision between VLBI and GPS carrier phase using IVS and IGS observation data in order to confirm the potential of VLBI time and frequency transfer. The results show that VLBI time transfer is more stable than GPS time transfer on the same baseline and same period.

1. Introduction

Modern cold-atom-based frequency standards have already archived the uncertainty of 10^{-15} at a few days. Moreover cold-atom-based optical clocks have the potential to realize the uncertainty on a 10^{-16} to 10^{-17} level after a few hours (Takamoto et al., 2005 [6]). On the other hand, time transfer precision of two-way satellite time and frequency transfer and GPS carrier phase experiments have reached the 10^{-10}@1sec (10^{-15}@1day) level (Ray and Senior, 2005 [5] etc.). In order to compare such modern standards by these time transfer techniques, it is necessary to average over long periods.

Since these techniques are not sufficient to compare next standards improvements of high precision time transfer techniques are strongly desired.

Very Long Baseline Interferometry (VLBI) is one of the space geodetic techniques measures the arrival time delays between multiple stations utilizing radio signals from distant celestial radio sources. By using VLBI, it is possible to measure subtle variations of Earth orientation parameters (EOP). In the usual geodetic VLBI analysis, clock offsets and their rates of change at each station are estimated with respect to a selected reference station. The averaged formal error (1 σ) of the clock offsets is typically about 20 picoseconds when analyzing geodetic VLBI experiments which are regularly conducted by the International VLBI Service for Geodesy and Astrometry (IVS). This precision is nearly one order better than other techniques like GPS or two-way satellite time transfer. It is feasible to use geodetic VLBI for comparison of primary frequency standards when radio telescopes are deployed at time and frequency laboratories. For this purpose, we have started to develop a compact and transportable VLBI system (Ishii et al., 2007 [2]).

To confirm the potential of the current VLBI time and frequency transfer aiming at the practical use in the future, we have compared the results of the VLBI and GPS carrier phase frequency transfer using Kashima-Koganei baseline (Takiguchi et al., 2007 [7]). That study showed that VLBI is more stable than GPS between 2000 seconds to 6000 seconds. In this study, we mainly compared VLBI and GPS carrier phase frequency transfer using data from the IVS and the International GNSS Service (IGS) by the same purpose.

2. The comparison experiments between VLBI and GPS carrier phase using IVS and IGS data

We checked the ability of time transfer of VLBI and GPS carrier phase using IVS and IGS data. We selected two stations (Onsala, Wettzell) which belong to IVS and IGS network. These two stations have in common that at each site VLBI and GPS are sharing the hydrogen maser (Figure 1). Table 1 shows a list of the data used for this study.

The details of the analysis of VLBI and GPS are listed as follows:

VLBI

- Software : CALC/SOLVE
- Strategy
    - multi baseline
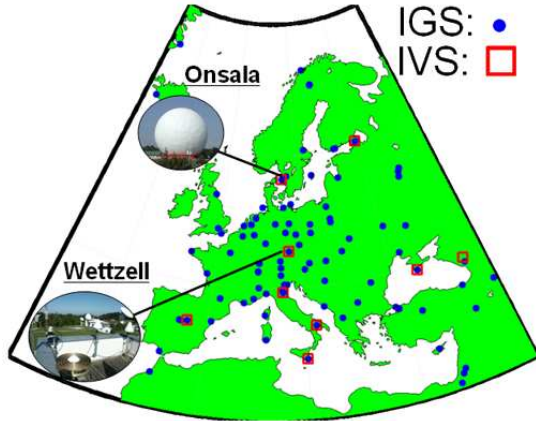   - S/X ionosphere-free linear combination
    - reference station: Wettzell

Figure 1. Map of IVS and IGS stations in Europe

Table 1. Data list

DOY	IVS		IGS
(2007)	Session	Station	Station
092	R1270		
100	R1271	ONSALA60,	onsa,
113	R1273	WETTZELL	wtzr
122	R1274		

- Estimate
  - station coordinates
  - atmospheric delay / 1h
  - clock offset / 1h

GPS

- Software : GIPSY-OASIS II
- Strategy
  - Precise Point Positioning (PPP) (Kouba and Heroux, 2001 [4])
- Estimate
  - station coordinates
  - atmospheric delay / 5min
  - clock offset / 5min
- Time Difference
  - *clock offset* A − *clock offset* B

Due to the code noise, the clock offsets of the GPS solutions show discontinuities at the day boundaries. The averaged day boundary discontinuity was 94ps. Figure 2 shows one of the VLBI results of clock offsets. The averaged formal errors (1 σ) of the estimated clock offsets at Onsala station referred to Wettzell station was 16.1ps.

Figure 3 shows that the time series of the clock difference between Onsala and Wettzell (session R1274) calculated from GPS and VLBI respectively (upper part). The lower part of Figure 3 is
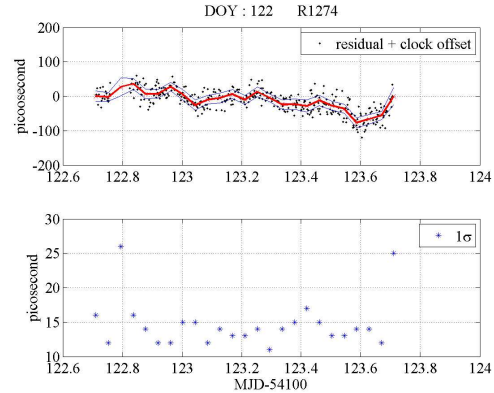
Figure 2. Time series of the clock offsets after removing linear trend (upper) and the formal error (lower) at Onsala station referred to Wettzell station.

the difference between GPS and VLBI clock offsets showing a good agreement within ±200ps.
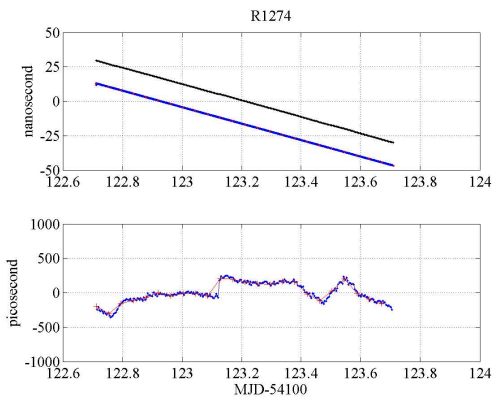

Figure 3. Time series of the clock difference (upper plot) calculated from GPS and VLBI respectively. The lower plot is the difference between GPS and VLBI clock offsets. The gap seen on 123(DOY) was caused by the day-boundary discontinuity of GPS.

Figure 4 and 5 illustrate the frequency stability of clock difference as obtained from VLBI and GPS. The short term stability of GPS carrier phase seems to be slightly better than those from VLBI for averaging periods up to 10^3s. However, VLBI is more stable at averaging periods longer than 10^3s in any sessions (Figure 5).

In general, the VLBI frequency transfer stability follows a $1/\tau$ law very close when averaging up to 10^4s. And that shows that the stability has reached about 2×10^{-11} (20ps) at 1 sec.
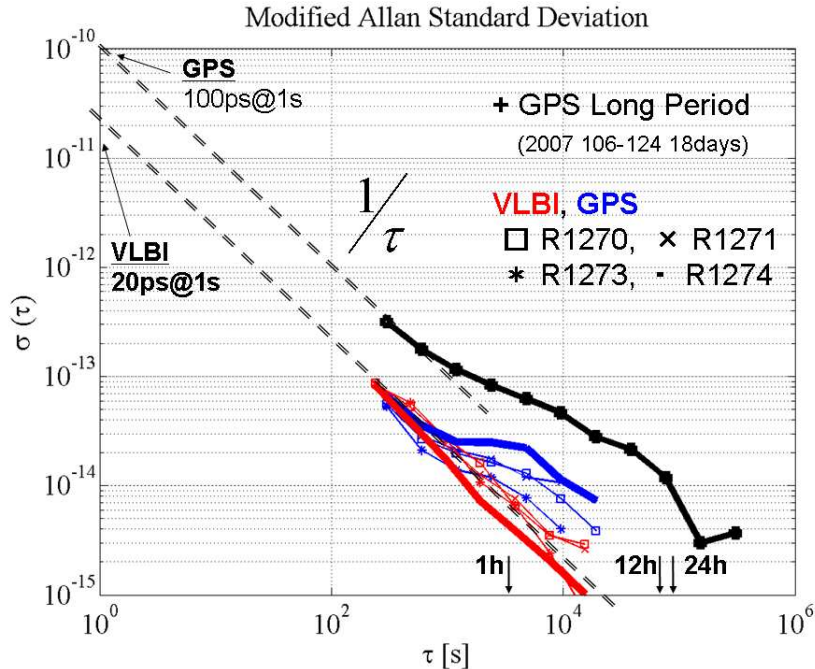
Figure 5. Modified Allan deviation of VLBI and GPS carrier phase results from all sessions.

Figure 4. Modified Allan deviation (top) and Time Standard Deviation (bottom) of VLBI and GPS carrier phase results from R1274 session.

3. The comparison experiments using KASHIMA-KOGANEI baseline

We also carried out geodetic VLBI experiments using Kashima-Koganei baseline in order to compare the results with GPS time transfer (carrier phase). We will also use this baseline for test observations of our compact VLBI system which is currently under development. The Kashima station which has a 34-m and a 11-m radio telescope, is located about 100 km East of Tokyo Japan. The Koganei station has a 11-m radio telescope, and is located in the western part of Tokyo. The baseline length is 109 km (Figure 6).

Both stations have a permanent GPS receiver (ksmv, kgni and ks34) which are sharing the H-maser with VLBI since last spring. It was necessary to adopt some parts of these VLBI and GPS equipment for the needs of the time and frequency transfer purpose because these systems are usually set-up for geodetic purposes.

At first, we carried out a test experiment with the unchanged systems. The details and data quality of the performed VLBI and GPS observations are listed in Table 2. The quality of the GPS observations was not good (except for the k08049 experiment) due to troubles with the GPS receivers. In the k08049 experiment we used a new GPS receiver (Trimble NetRS). In this paper, we discuss only k07166 and k08049 experiments.
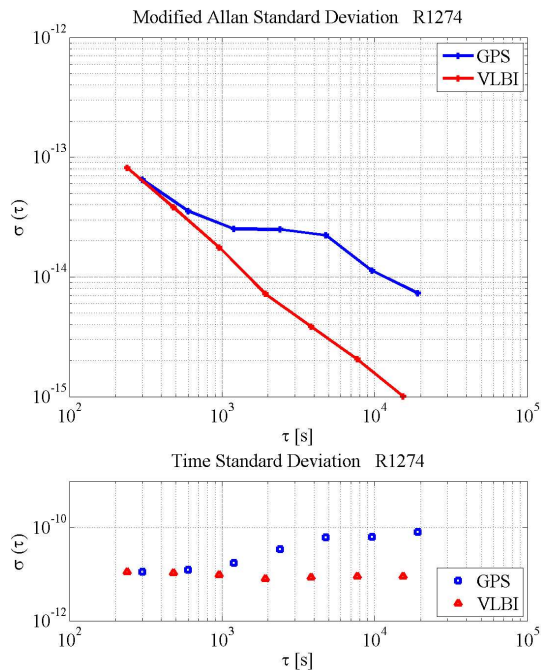
The analysis setup is almost the same as the one
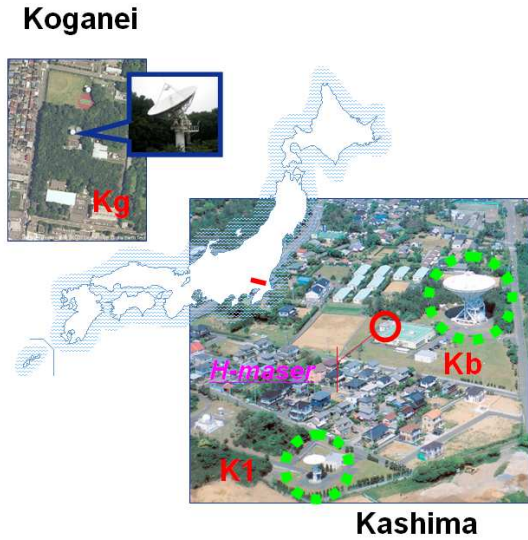
Koganei

Figure 6. *Layout map of KASHIMA and KO-GANEI station.*

Table 2. *Details of VLBI and GPS observations, which were dedicted to time and frequency transfer.*

Session	Baseline	Duration	Data Quality	
			VLBI	GPS
k07022	K1-Kg	24 hours	errors	errors
k07059	K1-Kg	3 days	errors	errors
k07166	Kb-Kg	1 week	OK	Failed
k08049	Kb-Kg	3 days	OK	OK

* K1: KASHIM11, Kg : KOGANEI, Kb : KASHIM34

described in the previous section. The averaged formal errors (1 σ) of the estimated clock offsets at Koganei station referred to Kashima station were 23ps (k07166) and 18ps (k08049) in VLBI results.

Figure 7 presents the comparison between VLBI and GPS. After removing a linear trend (lower plot), the clock offsets of VLBI reveal a diurnal variation which can not be seen in the GPS results. The cable length between the point where the reference signal from the H-maser is injected and the observing system itself is different for VLBI and GPS as shown in Figure 8. Additionally, the cable of the VLBI system inside the antenna is not temperature controlled. Figure 9 shows the time series of the clock offset of VLBI and the outside temperature. It reveals that the clock offsets of VLBI are strongly affected by the outside temperature (correlation coefficient : -0.72, *lag* : 2hours). Thus, for current experiments, we have decided to monitor variations of the reference signal through the transmission cable of the VLBI system by the Dual Mixer Time
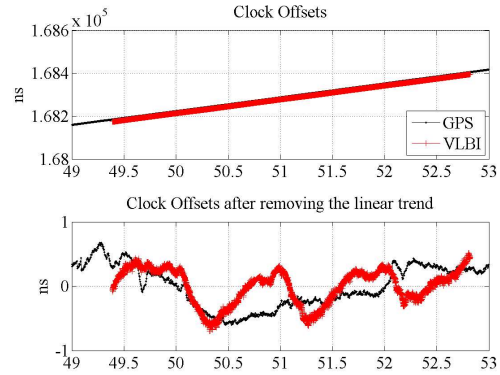

Figure 7. *Comparison between VLBI and GPS results (upper plot: clock offsets, lower plot: clock offsets after removing a linear trend).*

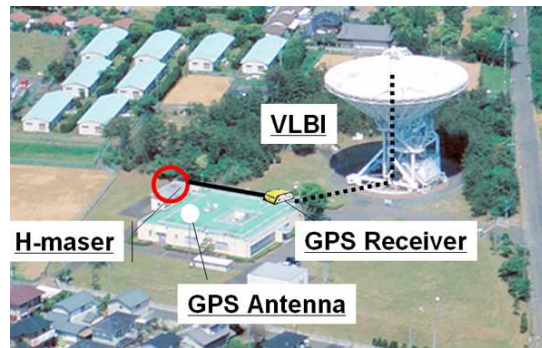Difference (DMTD) method (Komiyama, 1983 [3]).

Figure 8. *Layout of the H-maser, GPS receiver and VLBI antenna.*

These results suggest that it is necessary to calibrate the instrumental delay variation of the VLBI system. In the next step, we are planning to measure the instrumental delay of the VLBI system by the zero baseline interferometry (ZBI) method (Hama et al., 1986 [1], Yoshino et al., 1992 [8]), and we also want to replace the transmission cable by optical fibers.

4. Summary

To compare the results of VLBI and GPS (carrier phase) frequency transfer, we have analyzed IVS and IGS data. The results of the VLBI frequency transfer show that the stability follows a $1/\tau$ law very closely (phase noise dominant). And that shows the stability has reached about 2×10^{-11} (20ps) at 1 sec. In this study, the results show that VLBI frequency transfer is more stable than GPS on the same baseline and same period.
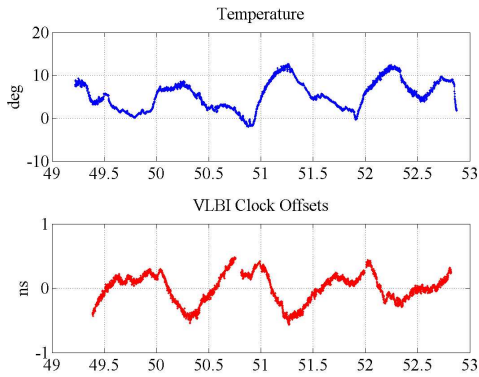
Figure 9. Time series of the outside temperature and clock offsets of VLBI.

Also, we prepared the setup on the Kashima-Koganei baseline for time and frequency transfer tests using our compact VLBI system which is currently under development. Figure 10 shows the future image of the time transfer by the compact VLBI system and high speed networks.
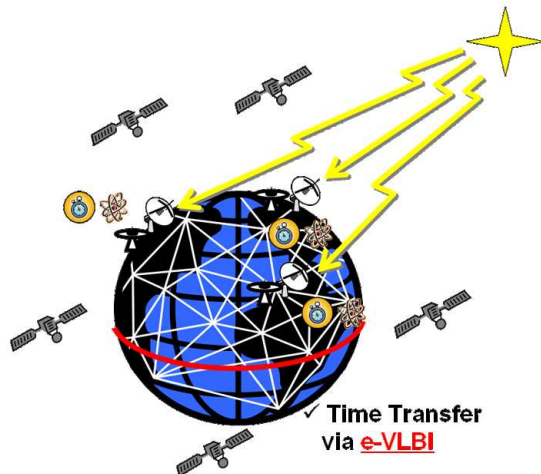

Figure 10. Future image of the time transfer by the compact VLBI system and high speed networks.

References

[1] Hama, S., H. Kiuchi, Y. Takahashi, J. Amagai, T. Yoshino, N. Kawaguchi, W. J. Klepczynski, and J. O. Martin, Japan-U.S. Time Comparison Experiment for Realizing Better Than 1-ns Accuracy by Using a Radio Interferometric Technique, *IEEE IM*, 38, 2, 640–643, 1989.

[2] Ishii, A., R. Ichikawa, H. Takiguchi, H. Kuboki, M. Kimura, J. Nakajima, Y. Koyama, J. Fujisaku, and K. Takashima, Development of a compact VLBI system for a length examination of a reference baseline, *IVS NICT-TDC News*, No.28, 2–5, 2007.

[3] Komiyama, B., Frequency and time measurement methods, *Radio Lab Bull*, Vol. 29, 39–53, 1983.

[4] Kouba, J., and P. Heroux, Precise Point Positioning using IGS orbits and clock products, *GPS Solutions*, No. 5, 12–28, 2001.

[5] Ray, J., and K. Senior, Geodetic techniques for time and frequency comparisons using GPS phase and code measurements, *Metrologia*, 42, 215–232, 2005.

[6] Takamoto, M., F.-L. Hong, R. Higashi, and H. Katori, An Optical Lattice Clock, *Nature*, 435, 321–324, 2005.

[7] Takiguchi, H., T. Hobiger, A. Ishii, R. Ichikawa, and Y. Koyama, Comparison with GPS Time Transfer and VLBI Time Transfer, *IVS NICT-TDC News*, No.28, 10–15, 2007.

[8] Yoshino, T., S. Hama, and H. Kiuchi, Precise Time Comparison with Very Long Baseline Interferometry, *J. of Com. Res. Lab.*, 39, 1, March, 1992.

Development of e-VLBI Technologies for Ultra-rapid UT1 Measurement

Mamoru Sekido[1](sekido@nict.go.jp),
Tetsuro Kondo[1], **Jan Wagner**[2],
Thomas Hobiger[1], **Kensuke Kokado**[3],
Hiroshi Takiguchi[1], **Yasuhiro Koyama**[1],
Rüdiger Haas[4], **Jouko Ritakari**[2]
and Shinobu Kurihara[3]

[1]*National Institute of Information and
   Communications technology, Kashima Space
   Research Center, 893-1, Hirai, Kashima,
   Ibaraki 314-8501, Japan*
[2]*Helsinki University of Technology, Metsähovi
   Radio Observatory, Metsähovintie 114
   FIN02540 Kylmälä, Finland*
[3]*Geographical Survey Institute, 1 Kitasato,
   Tsukuba 305-0811, Japan*
[4]*Chalmers University of Technology, Onsala
   Space Observatory, SE-439 92 Onsala, Sweden*

Abstract: Ultra-rapid UT1 measurements have been realized under the collaboration between NICT, GSI(Japan), Onsala Observatory(Sweden), and Metsähvi Radio Observatory(Finland). This achievement was made by a combination of software and hardware technologies with components of so called e-VLBI. This paper describes the components, which contributed the Ultra-rapid UT1 measurements.

1. Introduction

Orientation of solid Earth's crust with respect to the celestial reference frame is represented by polar motion and UT1. They change with time due to the interaction between gravitational forces of the Sun, Moon, Planets and responses of Earth's ocean, atmosphere, and the Earth's interior. The Earth orientation parameters (EOP) are still unpredictable with sufficient accuracy, although real-time use of them is required for several applications such as spacecraft navigation.

The IERS (International Earth Rotation and Reference Systems Service) and related institutes are making efforts and contributions for quick derivation of EOPs[7]. We have developed e-VLBI technologies, which enable real-time or pseudo real-time VLBI observation. A pilot project for quick measurement of UT1 by using e-VLBI has started as a collaboration between NICT, GSI (Geographical Survey Institute, Japan), Onsala Observatory (Chalmers Univ. of Tech., Sweden), and Metsähovi Radio Observatory (Helsinki Univ. Tech., Finland)

in April 2007. Since May 2007, UT1 measurement has become possible within 30 min. after the session. In February 2008, the fastest record of UT1 measurement within 4 minutes was achieved on Onsala-Tsukuba baseline[4]. The key technologies which enabled the Ultra-rapid UT1 measurement are introduced in the following sections.

2. e-VLBI Technologies

2.1 K5/VSSP32

NICT has developed a new PC-based VLBI data acquisition system named K5/VSSP32[3]. This is the second revision of K5/VSSP. Sampling rate has been expanded up to 32 Msps and data output interface has been changed to USB(Universal Serial Bus) instead of PCI-bus. One of the advantages
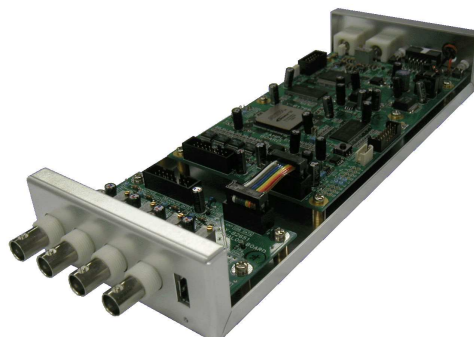
Figure 1. One unit of K5/VSSP32 has 4 channel input. A variety of sampling rates (40k,100k,200k,500k,1M,2M,4M,8M,16M,32M) and quantization bit (1,2,4,8) are available. Captured data are transfered to PC with USB(Universal Serial Bus) interface with maximum data rates up to 256 Mbps.

of the new system for e-VLBI is that simultaneous read/write access becomes available. Owing to this capability, the data can be processed soon after each scan has finished. Consequently data processing is performed during observation and the latency of VLBI observations has been greatly reduced.

2.2 High Speed Network and High Speed Protocol (Tsunami)

Real-time data transport from observatories in Scandinavian countries to Japan has been realized by high speed research network infrastructures. Research and educational network providers NOR-DUnet[1] and Géant2[2] are supporting the e-VLBI project in Europe. The data is coming through

---

[1]http://www.nordu.net/
[2]http://www.geant2.net/

Internet2[3] in the USA, and to Kashima 34m telescope via JGN2[4].

VLBI observations essentially require long distance data transport with high data rate. The network path length from Scandinavian stations (Onsala, and Metsähovi) to Japanese stations (Kashima and Tsukuba) is over twenty thousands km. TCP/IP, which is a protocol widely used on the Internet, has not enough performance to transfer the data with a data rate over a 256Mbps or 512Mbps over such a distance. Meiss[5] of Indiana Univ. developed a UDP(user datagram protocol)-based data transport protocol 'Tsunami' for high speed file transport on high latency networks. J.Wagner and J.Ritakari at Metsähovi observatory[5] have improved and adapted it for real-time VLBI data transfer. VLBI data output from Mark5 formatter is captured by a PC-based data acquisition interface card (VSIB) developed by Metsähovi[6]. Then the data are transfered by the 'real-time Tsunami' software. 'Tsunami' protocol has proven the performance of data transfer rate over 600 Mbps on the Metsähovi (Finland) - Kashima (Japan) baseline. Thanks to the high speed research (shared) network and real-time Tsunami protocol, observed data at Scandinavian stations are recorded in Mark5-A format[9] at Kashima in real-time. Following to the data transfer, data format conversion and correlation processes are automatically performed.

2.3 Software Correlator and Automatic Processing

VLBI data observed at Scandinavian stations are transported and recorded at the Japanese side (Kashima or Tsukuba) in real-time. Data format conversion from Mark5 to K5/VSSP is performed automatically in accordance with the observation schedule file. The K5/VSSP software package[2] has been used for the data conversion and software correlation. Since the modules in that package do not have a function to communicate with each other, a simple distributed computing environment has been developed. It is composed of task manager and job processing agents. Each of them runs as a process and communicates via TCP/IP. By using such a task shared environment, data format conversion, correlation processing, and bandwidth synthesis procedures are performed as a pipeline. Each component of the manager/agent subsystem is coded by the script language *Perl*. A principle for designing the task-sharing system was *"Minimum mutual dependency"*. This pol-

icy was intended to minimize the impact of failures/troubles at single task on the whole processing scheme. Each component is designed to work independently. This allows also to maintain the components easily. *Perl* language was chosen because it is TCP/IP friendly and it has large archive database of modules (CPAN) with a variety of functions. The main task of the subsystem is to manage the computer resources and delivering jobs. Figure 2 shows an overview of the pipeline data processing scheme for the distributed computing environment.

After correlation processing has finished, bandwidth synthesis is performed to derive precise group delay observables.

2.4 MK3TOOLS and UT1 Analysis

After the correlation processing, the data were analyzed in two ways by using VLBI analysis software CALC/SOLVE and OCCAM. The CALC/SOLVE uses MK3 databases whereas OCCAM uses NGS cards as input of VLBI data. Hobiger et al.[1] have developed a VLBI database system based on NetCDF (network Common Data Form)[6] as a tool for storing and retrieving VLBI data. By using the MK3TOOLS, VLBI data in either MK3 database or NGS card formats can be generated. VLBI database for geodesy are stored in MK3 database form in most cases, though MK3 databases have a strong dependency on computer hardware and it has not been designed for standard Linux systems. Therefore VLBI database handling with MK3TOOLS has the great advantage, that VLBI data can be manipulated on any computer platforms.

In our ultra-rapid UT1 measurement, the MK3TOOLS have been used for the creation of MK3 databases and NGS cards for analysis with CALC/ SOLVE and OCCAM. Automatic UT1 estimation scheme has been developed by T.Hobiger using OCCAM. Iterative ambiguity solution and UT1 estimation has been performed automatically. Manual UT1 analysis with CALC/SOLVE has been also used as another way. The typical latency of UT1 measurement is 25 min., 40min., and 100 min. for total data rates at 128, 256, and 512 Mbps, respectively. The current bottle neck of the data processing at high data rate is the data format conversion of raw VLBI data from Mark5 to K5/VSSP. We are going to improve this point in the near future.

3. Summary

The pilot project of Ultra-rapid UT1 measurement with e-VLBI has been operated success-

---

[3]http://www.internet2.edu/
[4]http://www.jgn.nict.go.jp/
[5]http://www.metsahovi.fi/en/vlbi/soft-tools/

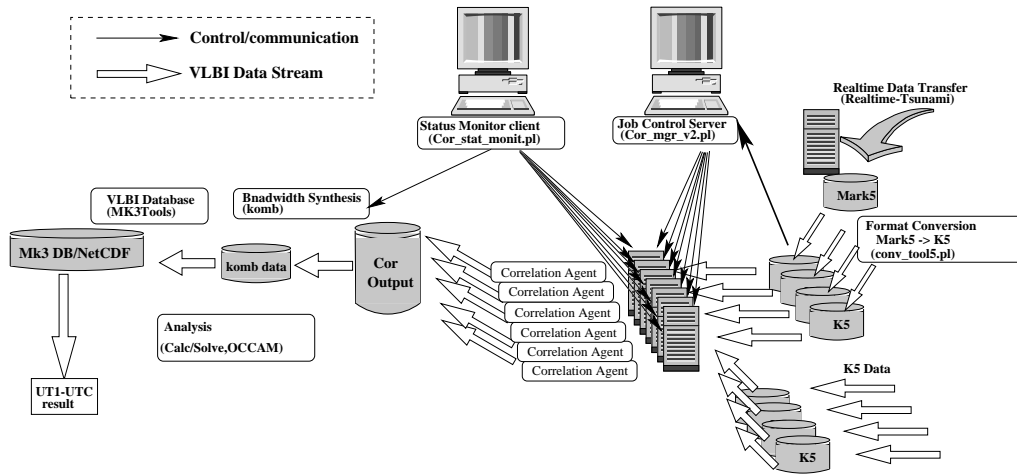[6]http://www.unidata.ucar.edu/software/netcdf/

Figure 2. Automatic data processing with distributed computing environment. The software correlator and data format converter are used fro pipeline data reduction of the VLBI data.

fully under a collaboration between Scandinavian (Onsala, Metsähovi) and Japanese (Kashima, Tsukuba) VLBI stations. The quick UT1 measurements are enabled by international high speed network infrastructures (Géant2, JGN2, Internet2,...), high speed data transport protocols (real-time Tsunami), and PC-based data acquisition systems (K5,Mark5,VSIB). Computing power of personal computer is now capable of handling raw VLBI data by software. This leads to an improvement of compatibility of the systems and helps to boost data conversion between different VLBI data formats. Thus mutual collaboration will be enhanced with e-VLBI and a further expansion of VLBI networks is expected.

References

[1] Hobiger, T., Y. Koyama, T. Kondo, "MK3TOOLS & NetCDF – storing VLBI data in a machine independent array oriented data format", *Proceeding 18th European VLBI for Geodesy and Astrometry (EVGA) Working Meeting April 12-13, 2007, Vienna, Austria, (http://mars.hg.tuwien.ac.at/ẽvga/)*, P03, 2007.

[2] Kondo, T., Y. Koyama, H. Takeuchi, and M. Kimura, "Current Status of the K5 Software Correlator", *IVS NICT-TDC News*, No. 25, pp. 23-27., 2004.

[3] Kondo, T., Y. Koyama, H. Takeuchi, and M. Kimura, "Development of a New VLBI Sampler Unit (K5/VSSP32) Equipped with a USB 2.0 Interface", *IVS 2006 General Meeting Proceedings(eds. Dirk Behrend & Karen Baver)*, NASA/CP-2006-214140, pp. 195-199, 2006.

[4] Matsuzaka, S,, K. Wada, S. Kurihara, Y. Koyama, M. Sekido, R. Haas, and J. Wagner, "Ultra-rapid UT1 Measurements with e-VLBI", in Proceedings of the 5th IVS General Meeting, St. Petersburg March 3-6, 2008.

[5] Meiss, M, "Tsunami: A High-Speed Rate-Controlled Protocol for File Transfer", http://steinbeck.ucs.indiana.edu/m̃meiss/ papers/tsunami.pdf, 2004.

[6] Ritakari, J., and A. Mujunen, "Gbit/s VLBI and eVLBI with Off-The-Shelf Components", *International VLBI Service for Geodesy and Astrometry 2004 General Meeting Proceedings (eds. Nancy R. Vandenberg & Karen D. Baver)*, NASA/CP-2004-212255, pp. 182–185, 2004.

[7] Rothacher, M., D. Thaller, and R. Dill, "Analysis Coordinator", *IERS Annual Report 2005*, pp. 29-31., 2005.

[8] Sekido, M., H. Takiguchi, Y. Koyama, T. Kondo, R. Haas, J. Wagner, J. Ritakari, S. Kurihara, and K. Kokado, "Ultra-rapid UT1 measurement by e-VLBI", *Earth Planets and Space*, in print 2008.

[9] Whitney, A., "Mark IIIA/IV/VLBA Tape Formats, Recording Modes and Compatibility", Mark IV Memo series 230A, http://www.haystack.mit.edu/geo/mark4/memos /230.pdf, 2000.

Real-time ray-tracing through numerical weather models for space geodesy

Thomas Hobiger (*hobiger@nict.go.jp***),
Ryuichi Ichikawa, Yasuhiro Koyama,
and Tetsuro Kondo**

*Kashima Space Research Center, National
Institute of Information and Communications
Technology, 893-1 Hirai, Kashima, Ibaraki
314-8501, Japan*

Abstract: Numerical weather models have under-
gone an improvement of spatial and temporal res-
olution in the recent years, which made their
use for space geodetic applications feasible. Ray-
tracing through such models permits the compu-
tation of total troposphere delays and ray-bending
angles. At the National Institute of Information
and Communications Technology (NICT) the so-
called KAshima RAy-tracing Tools (KARAT) have
been developed which allow to obtain troposphere
delay corrections in real-time. Together with fine-
mesh weather models from the Japanese Meteoro-
logical Agency (JMA) huge parts of the East Asian
region, including Japan, Korea, Taiwan and East
China, can be covered. Thus a short overview
about the capabilities and functions of KARAT
will be given and computation performance issues
will be discussed. The ray-traced total troposphere
slant delays can be used as a correction of space
geodetic data on the observation level. Addition-
ally, an overview will be given about the upcoming
on-line service, which permits the reduction of tro-
posphere delays from user-submitted data.

1.   Introduction

The introduction of new mapping functions
(e.g. *Niell* (1996[7],2001[8]), *Boehm et al.*(2006a[1],
2006b[2])) in the recent years significantly im-
proved space geodetic techniques. Although mod-
ern mapping functions are derived from numerical
weather models the information from such mete-
orological data-sets is reduced to a few time- and
location-dependent coefficients which relate slanted
troposphere quantities to equivalent zenith mea-
sures. Moreover, the spatial variations of the tropo-
sphere above each station have to be estimated in
the analysis process in the form of gradient parame-
ters. As numerical weather models of regional size
have undergone an improvement of accuracy and
precision it became feasible to utilize ray-traced
troposphere slant delays directly for the geodetic
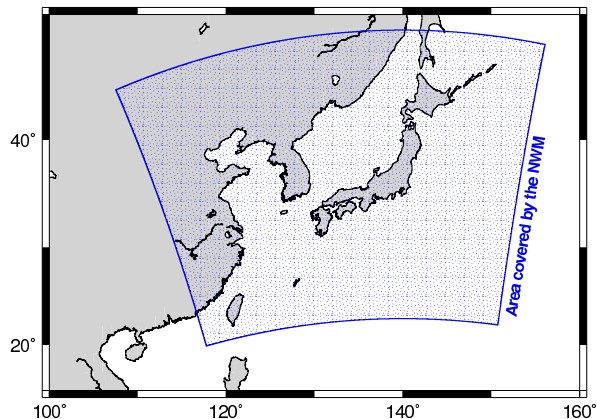analysis of space geodetic techniques.

*Figure 1. The spatial domain for which JMA meso-
scale weather models are available.*

1.1   Mesoscale analysis models from the JMA

The Japanese Meteorological Agency (JMA)
provides a variety of weather models ranging from
global models to fine-mesh models which cover
an area of only a few tens of kilometers. The
meso-scale 4D-Var model (i.e. Meso-scale Anal-
ysis Data (MANAL)) from JMA (*JMA*(2002)[6],
Ishikawa(2001)[5]) with its horizontal resolution of
about 10km was found to have the best trade-off
between grid-spacing and area size. This model
covers large parts of Eastern Asia, including Japan
and its Southern islands, Korea, Taiwan and East-
ern China (figure 1). Moreover, the three hour
time-resolution of the data-sets makes the appli-
ance of this model for positioning applications fea-
sible.

2.   Kashima ray-tracing tools (KARAT)

Based on the requirement to deliver ray-traced
delays in real-time (assuming that numerical
weather models are available as forecast data) a set
of tools have been created in order to carry out the
ray-tracing tasks. Coding in C++ does not only
permit to design the modules close to machine lan-
guage, but also allows to interface external classes
which enable multi-core/multi-processor support.
A detailed description about KARAT and its per-
formance can be found in *Hobiger et al.* (2008b)[4].

2.1   Preparing the data

Since the grid points of the JMA mesoscale
weather models are not equally spaced on a geo-
graphic coordinate system it is necessary to inter-
polate them on a rectangular grid. Moreover, it is
mandatory to transform the geopotential heights,
which are used by the meteorologists, into geomet-
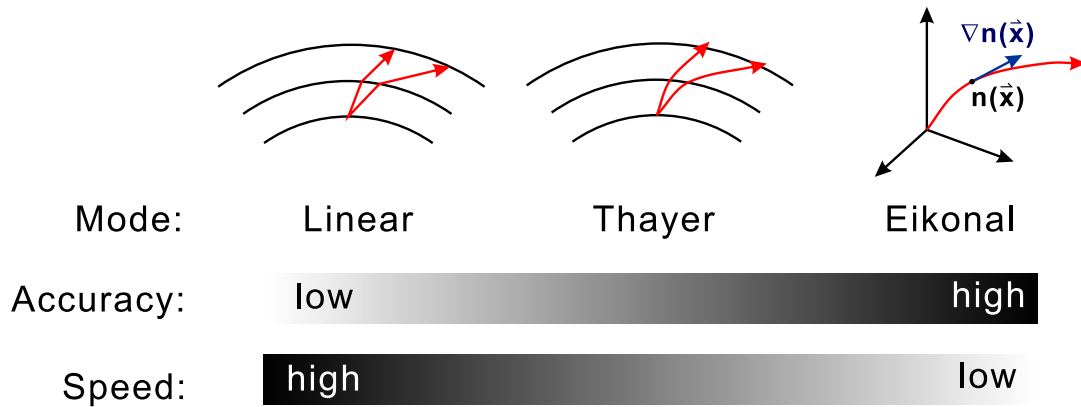ric heights, which can be used for ray-tracing calcu-

Figure 2. The three ray-tracing modes of KARAT together with their accuracy and speed performance.

lations. Thus, the first tool of KARAT handles all this tasks, using a sophisticated interpolation algorithm which allows to compute refractivity values on a geographic grid with user-defined boundaries, resolution and height steps. Each epoch of the numerical weather model is processed by this tool and binary files are created for follow-on processing. As described by *Hobiger et al.* (2008b)[4], a dedicated height system helps to reduce the number of necessary height levels without accuracy degradation of the ray-traced slant delays.

2.2 The ray-tracer

The main module of KARAT is the ray-tracing engine which reads consecutive binary weather models, covering a 24 hours period and loads the refractivity fields into free memory. Once all the data is put to memory, ray-tracing cores can be launched independently. Each core is at idle status until station position and ray-geometry (i.e. time, azimuth and elevation angles) are parsed to it. As KARAT uses OpenMP (e.g. *Quinn*(2004)[9]) to take advantage of multi-core and multi-processor architectures, the number of available ray-tracing cores is only limited by the number of CPU cores which share the same memory. KARAT offers three different modes (figure 2) in which the ray-tracing can be carried out.

he fastest, but least accurate one assumes linear ray-propagation between two height levels and computes the refraction when the ray-crosses a layer. The more advanced mode, considers that the ray is also bended when propagating between two levels. This mode is called Thayer, named after the corresponding paper by *Thayer*(1976)[10]. Both modes fully consider the 3D refractivity field, but don't allow for out-of-plane propagation of the ray. The most sophisticated, but also slowest mode solves the Eikonal equation numerically and pro-

vides the 3D ray-path together with the total delay. As the differences between the Thayer and the Eikonal model hardly exceeds the mm-level at lowest elevations (3 degrees) the Thayer mode is often selected as a compromise between speed and accuracy.

The ray-tracing module allows to handle geometry files (i.e. text files containing site positions, epochs, azimuth and elevation angles) or reads RINEX files and computes the observing geometry using IGS orbit information. Moreover the reduction of troposphere delays is supported by correcting code and phase measurements directly in the RINEX files.

2.3 Supporting tools

Beside the main modules described above, KARAT includes smaller tools for the manipulation of (binary) numerical weather models as well as scripts for orbit calculations and display of the results. It is planned for the future that an additional module will manage large ray-tracing jobs and distribute the work-load on several ray-tracing clients.

3. Ray-traced troposphere for space geodesy - first results

Hobiger et al. (2008a)[3] have analyzed the impact of ray-traced troposphere delays on precise point positioning with GPS. As the numerical weather models currently don't allow to obtain mm-accurate slant troposphere delays, it was necessary to estimate a residual troposphere delay, when using ray-traced data-sets. Station height repeatabilities of several GPS sites in East Asia could be improved when KARAT data has been used. Moreover the RMS of the residuals were found to be at the same levels as those obtained
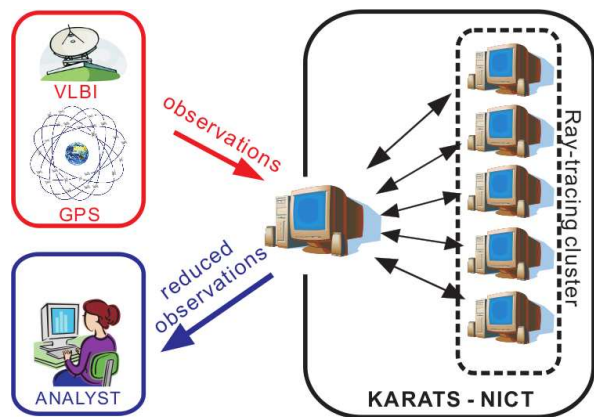
Figure 3. Flow chart of the KARATS processing chain. KARATS will subtract troposphere delays from the user's observation based on the geometry computed from precise orbits(GNSS) or source positions (VLBI).

from modern mapping functions and gradient estimation. Additionally, the authors could show that positioning solutions with cm-range accuracy could be achieved when the ray-traced data was analyzed without residual troposphere estimation.

In order to apply such corrections to VLBI measurements it is necessary that both stations are either within the same high-resolution weather model or that several regional numerical weather models are used to consider the weather conditions at each site. Although KARAT is currently only dealing with meso-scale data from JMA it is possible to handle numerical weather models from other weather agencies. Tests with ray-traced troposphere slant delays for East Asian VLBI networks are planned for the close future.

4. Kashima ray-tracing service (KARATS)

In order to enable users of space geodetic techniques to take advantage from KARAT without the need to access numerical weather models by their own it was decided to provide ray-tracing as a service. Thus the ray-tracing tools will be embedded in an automatic processing chain, called Kashima Ray-Tracing Service (KARATS), which can be started via a web-interface. Figure 3 shows how KARATS is expected to operate. Once a user (from the GPS or VLBI community) has taken his observations, he can send the data in a common format (which will be RINEX for GPS and MK3/FITS for VLBI at first) via Internet to KARATS. Thereafter the web-server will do a rough data-check and compute the geometry from the observation file. As soon as a ray-tracing client becomes available it will send the geometry file to

that machine. The client performs the ray-tracing through the weather model and sends the tropospheric delays back to the server. Thereafter the ray-traced delays are subtracted from the user's data and a "reduced" observation file is sent back to the user. Thus the analyst can estimate his target parameters without spending too much effort on estimating tropospheric delays. In the case that VLBI observations are submitted it is checked that both stations lie within the boundaries of the NWM and thereafter the tropospheric delays are computed at each station. In a final step the server will compute the differenced corrections and apply them to the VLBI observations.

Moreover it is planned to run KARATS for real-time applications. Since this mode needs weather prediction data from the JMA it will be limited to a selected user group. The KARATS post-processing mode will be free of charge and a turn-around time of one minute per (RINEX) file is anticipated.

References

[1] Boehm, J., A. Niell, P. Tregoning, and H. Schuh (2006a), Global Mapping Function (GMF): A new empirical mapping function based on numerical weather model data, *Geophys. Res. Lett.*, **33**, L07304, doi:10.1029/2005GL025546.

[2] Boehm, J., B. Werl, and H. Schuh (2006b), Troposphere mapping functions for GPS and very long baseline interferometry from European Centre for Medium-Range Weather Forecasts operational analysis data, *J. Geophys. Res.*, **111**, B02406, doi:10.1029/2005JB003629.

[3] Hobiger T., R. Ichikawa, T. Takasu, Y. Koyama and T. Kondo (2008a), Ray-traced troposphere slant delays for precise point positioning, *Earth, Planets and Space*, **60**, e1–e4.

[4] Hobiger T., R. Ichikawa, Y. Koyama and T. Kondo (2008b), Fast and accurate ray-tracing algorithms for real-time space geodetic applications using numerical weather models, *J. Geophys. Res.*, doi:10.1029/2008JD010503, in press.

[5] Ishikawa, Y., Development of a mesoscale 4-dimensional variational data assimilation (4D-Var) system at JMA, *Proceedings of the 81st Annual Meeting of the AMS: Precipitation Extremes: Prediction, Impacts and Responses*, P2.45, 2001.

[6] JMA, Outline of the operational numerical weather prediction at the Japanese Meteorological Agency, 158pp, 2002.

[7] Niell, A. E. (1996), Global mapping functions for the atmosphere delay at radio wavelengths, *J. Geophys. Res.*, **101**(B2), 3227–3246.

[8] Niell, A. E. (2001), Preliminary evaluation of atmospheric mapping functions based on numerical weather models, *Phys. Chem. Earth*, **26**, 475–480.

[9] Quinn, M. J. (2004), Parallel Programming in C with MPI and OpenMP, McGraw-Hill Inc,.

[10] Thayer, G. (1967), A rapid and accurate ray tracing algorithm for a horizontally stratified atmosphere, *Radio Science*, **1**, pp. 249–252.

Figure 4. Logo of KARATS.